

On the implied volatility of European and Asian call options under the stochastic volatility Bachelier model

Elisa Alòs*, Eulàlia Nualart*, and Makar Pravosud*

August 30, 2023

Abstract

In this paper we study the short-time behavior of the at-the-money implied volatility for European and arithmetic Asian call options with fixed strike price. The asset price is assumed to follow the Bachelier model with a general stochastic volatility process. Using techniques of the Malliavin calculus such as the anticipating Itô's formula we first compute the level of the implied volatility when the maturity converges to zero. Then, we find a short maturity asymptotic formula for the skew of the implied volatility that depends on the roughness of the volatility model. We apply our general results to the SABR and fractional Bergomi models, and provide some numerical simulations that confirm the accurateness of the asymptotic formula for the skew.

Keywords: Bachelier model, Stochastic volatility, European options, Asian options, Malliavin calculus, implied volatility

1 Introduction

The life of quantitative finance and derivatives pricing has started when Louis Bachelier presented an option pricing model in his Ph.D. thesis [6]. However, the suggested model is arithmetic and allows negative asset prices, as a result, the Bachelier model has not gained popularity. Until recently the model has not been widely studied in the literature and applied in practice. Nowadays option pricing models are strongly based on the Black-Scholes model. Local, stochastic and even fractional volatility models (see Alòs and Lorite [2] for an introduction to these topics) are extensions of the Black-Scholes model, where the volatility is allowed to be a function of the price of the stock price (local), a diffusion process (stochastic) or a function of a fractional Brownian motion (fractional). As the Black-Scholes model is a geometric Brownian motion (following a log-normal distribution), all the above models are also exponentials of random variables, and they share the positivity of the stock price. This plausible and intuitive property has been assumed for a long time for the prices of the underlying asset of an option.

From a practical perspective, the Bachelier model has started to gain more attention when negative prices have been registered, for example, on April 20th 2020, when crude oil futures crossed the zero mark and took negative values. As a prompt response to enable markets to continue to function normally, the CME Clearing started to use the Bachelier model to cope with negative underlying prices. The empirical paper by Galeeva and Ehud [11] studies the turbulent period on the oil-futures options markets which was observed in the middle of

*Universitat Pompeu Fabra and Barcelona School of Economics, Department of Economics and Business, Ramón Trias Fargas 25-27, 08005, Barcelona, Spain. EN acknowledges support from the Spanish MINECO grant PGC2018-101643-B-I00 and Ayudas Fundacion BBVA a Equipos de Investigación Científica 2017.

February 2020. The authors analyzed the observed implied volatilities by applying the Bachelier and Black models to prevail oil-futures option prices.

Apart from the energy market, the Bachelier model is also used in modelling interest rate products, for example, Euro denominated caps. The detailed analysis on the reasons to use a normal model rather than a log-normal one in the case of interest rates is presented in Goodman [12]. The recent paper by Choi et al. [7] is a comprehensive review of various topics related to the Bachelier model for both researchers and practitioners. In particular, they cover topics such as the implied volatility inversion problem, volatility conversion between related models, Greeks and hedging, as well as pricing of exotic options.

Concerning exact analytical results, in the paper by Schachermayer and Teichmann [15], the authors compare the option pricing problem under the Bachelier and Black-Scholes models. They find that prices coincide very well and explain by the means of chaos expansion theory why the Bachelier model yields good short-time approximations of prices and volatilities. In addition to that, the computation of prices and implied volatilities under the Bachelier model model has been presented in, for example, Terkado [16]. However, the existing literature lacks the rigorous analysis of the behaviour of the ATM level and skew of the implied volatility under the Bachelier model with stochastic volatility. By contrast, in the case of a regular Black-Scholes framework, there are numerous papers that study the short end maturity behaviour of the implied volatility under a variety of models such as the Heston, the SABR and fractional Begomi. For example, see Alòs [4], Figueroa-López et al. [8], Fukasawa [10], Fouque et al. [9].

The goal of this paper is to fill the gap in the existing literature and to analyze the option pricing problem when we allow the volatility of the Bachelier model to be a stochastic process. That is, to study option prices and implied volatilities for local, stochastic and fractional Bachelier models, both for vanilla and for exotic, in particular, Asian options. Specifically, we present analytical results for the behaviour of the level and the skew of the implied volatility for a general stochastic volatility Bachelier model. Our main tool for proving these results is Malliavin calculus, see Appendix A for an introduction to this topic. Additionally, using the findings from the theoretical part of the paper we do an extensive numerical simulations to investigate the quality of the first order approximations of the implied volatility across different moneyness and maturity scenarios. The presented results are extension of the papers Alòs [1], Alòs et.al [3] and Alòs, Nualart, Pravosud [5].

The paper is organized as follows. Section 2 is devoted to the statement of the problem and main results. Intermediary steps and the proofs of the main results are presented in Sections 3 and 4. Finally, in Section 5 we present and discuss the results of the numerical study.

2 Statement of the problem and main results

Let $T > 0$ and consider the following model for asset prices S (without lost of generality, we take the interest rate equal to zero for the sake of simplicity) in a time interval $[0, T]$

$$\begin{aligned} dS_t &= \sigma_t dW_t \\ W_t &= \rho W'_t + \sqrt{1 - \rho^2} B_t, \end{aligned} \tag{1}$$

where $S_0 > 0$ is fixed, W_t , W'_t , and B_t are three standard Brownian motions on $[0, T]$ defined on the same risk-neutral complete probability space $(\Omega, \mathcal{G}, \mathbb{P})$. We assume that W'_t and B_t are independent and $\rho \in [-1, 1]$ is the correlation coefficient between W_t and W'_t , and that σ_t is an a.s. continuous and square integrable process adapted to the filtration generated by W'_t . We denote by \mathbb{E}_t the conditional expectation with respect to the filtration generated by W_t .

Observe that when the volatility σ is constant, equation (1) is the classical Bachelier model. Notice that, in this case, asset prices are normally distributed.

We consider the following hypotheses on the volatility of the asset price. These hypotheses have been taken for the sake of simplicity and can be replaced by adequate integrability conditions.

Hypothesis 1. *There exist positive constants c_1 and c_2 such that for all $t \in [0, T]$,*

$$c_1 \leq \sigma_t \leq c_2.$$

Hypothesis 2. *For $p \geq 2$, $\sigma \in \mathbb{L}_{W'}^{2,p}$.*

Hypothesis 3. *There exists $H \in (0, 1)$ and for all $p \geq 1$ there exist constants $c_1, c_2 > 0$ such that for all $0 \leq s \leq r \leq u \leq T \leq 1$*

$$\{\mathbb{E}(|D_r^{W'} \sigma_u|^p)\}^{1/p} \leq c_1(u - r)^{H - \frac{1}{2}} \quad (2)$$

and

$$\{\mathbb{E}(|D_s^{W'} D_r^{W'} \sigma_u|^p)\}^{1/p} \leq c_2(u - r)^{H - \frac{1}{2}}(u - s)^{H - \frac{1}{2}}. \quad (3)$$

We denote by $(V_t^E)_{t \in [0, T]}$ the value of a European call option with fixed strike k . In particular,

$$V_T^E = \mathbb{E}(S_T - k)_+.$$

In a similar way, we denote by $(V_t^A)_{t \in [0, T]}$ the price of an arithmetic Asian call option with fixed strike k . Then

$$V_T^A = \mathbb{E}(A_T - k)_+,$$

where $A_T = \frac{1}{T} \int_0^T S_t dt$.

In order to deal with Asian options we follow the same approach as in [3], that is, we consider the martingale $M_t = \mathbb{E}_t(A_T)$. Applying the stochastic Fubini's theorem we get that

$$\begin{aligned} A_T &= \frac{1}{T} \int_0^T S_t dt = \frac{1}{T} \int_0^T \left(S_0 + \int_0^t \sigma_u dW_u \right) dt = \\ &= S_0 + \frac{1}{T} \int_0^T \sigma_u \left(\int_u^T dt \right) dW_u. \end{aligned}$$

This implies that

$$dM_t = \frac{\sigma_t(T-t)}{T} dW_t = \phi_t dW_t, \quad (4)$$

where

$$\phi_t := \frac{\sigma_t(T-t)}{T}.$$

Notice that, under the classical Bachelier model, A_T is a Gaussian random variable with mean S_0 and variance $\frac{\sigma^2 T}{3}$.

We denote by $B_E(t, S_t, k, \sigma)$ the classical Bachelier price of a European call option with time to maturity $T - t$, current stock price S_t , strike price k and constant volatility σ . That is,

$$B_E(t, S_t, k, \sigma) = (S_t - k)N(d_E(k, \sigma)) + n(d_E(k, \sigma))\sigma\sqrt{T-t},$$

where

$$d_E(k, \sigma) = \frac{S_t - k}{\sigma\sqrt{T-t}}.$$

Here N and n denote the cumulative distribution function and the probability density function of a standard normal random variable, respectively. Additionally, we recall that the Bachelier price satisfies the following PDE

$$\partial_t B_E(t, x, k, \sigma) + \frac{1}{2} \sigma^2 \partial_{xx}^2 B_E(t, x, k, \sigma) = 0. \quad (5)$$

Similarly, we denote by $B_A(t, S_t, y_t, k, \sigma)$ the Bachelier price of an arithmetic Asian call option with constant volatility σ , where $y_t = \int_0^t S_u du$. A direct computation shows that (see the Appendix for the details)

$$B_A(t, S_t, y_t, k, \sigma) = \left(S_t \frac{T-t}{T} + \frac{y_t}{T} - k \right) N(d_A(k, \sigma)) + \left(\frac{\sigma(T-t)\sqrt{T-t}}{T\sqrt{3}} \right) n(d_A(k, \sigma)),$$

where

$$d_A(k, \sigma) = \frac{S_t \frac{T-t}{T} + \frac{y_t}{T} - k}{\left(\frac{\sigma(T-t)\sqrt{T-t}}{T\sqrt{3}} \right)}.$$

Notice that we have the relation

$$B_A(t, S_t, y_t, k, \sigma) = B_E \left(t, M_t, k, \frac{\sigma(T-t)}{T\sqrt{3}} \right).$$

We next define the implied volatility (IV) of a European call option as the quantity $I_E(t, k)$ such that

$$V_t^E = B_E(t, S_t, k, I_E(t, k)),$$

and we denote by $I_E(t, k_t^*)$, where $k_t^* = S_t$, the corresponding at-the-money implied volatility (ATMIV) which, in the case of zero interest rates, takes the form $B_E^{-1}(t, S_t, S_t, V_t^E)$. Similarly, we define the implied volatility of an Asian call option $I_A(t, k)$ as the quantity such that

$$V_t^A = B_A(t, S_t, y_t, k, I_A(t, k)),$$

and we denote by $I_A(t, k_t^*)$ the corresponding ATMIV which, in the case of zero interest rates, takes the form $B_A^{-1}(t, S_t, y_t, S_t \frac{T-t}{T} + \frac{y_t}{T}, V_t^A)$. We set $k^* = k_0^*$.

The aim of this paper is to apply the Malliavin calculus techniques developed in Alòs [4] and Muguruza et al. [3] in order to obtain formulas for the ATMIV level and skew as $T \rightarrow 0$ under the general stochastic volatility model (1).

The main result of this paper is the following theorem.

Theorem 1. *Assume Hypotheses 1-3. Then,*

$$\lim_{T \rightarrow 0} I_E(0, k^*) = \sigma_0 \quad \text{and} \quad \lim_{T \rightarrow 0} I_A(0, k^*) = \sigma_0. \quad (6)$$

Moreover,

$$\begin{aligned} & \lim_{T \rightarrow 0} T^{\max(\frac{1}{2}-H, 0)} \partial_k I_E(0, k^*) \\ &= \lim_{T \rightarrow 0} T^{\max(\frac{1}{2}-H, 0)} \frac{\rho}{\sigma_0 T^2} \int_0^T \int_r^T \mathbb{E}(D_r^{W'} \sigma_u) du dr \end{aligned} \quad (7)$$

and

$$\begin{aligned} & \lim_{T \rightarrow 0} T^{\max(\frac{1}{2}-H, 0)} \partial_k I_A(0, k^*) \\ &= \lim_{T \rightarrow 0} T^{\max(\frac{1}{2}-H, 0)} \frac{9\rho}{\sigma_0 T^5} \int_0^T (T-r) \int_r^T (T-u)^2 \mathbb{E}(D_r^{W'} \sigma_u) du dr, \end{aligned} \quad (8)$$

Observe that when prices and volatilities are uncorrelated then the short-time skew equals to zero, which coincides with the constant volatility case. Notice also that if the term $\mathbb{E}(D_r^{W'} \sigma_u)$ is of order $(u-r)^{H-\frac{1}{2}}$, the limit of the right hand side of (7) will be 0 if $H > 1/2$ and it will converge to a constant when $H = \frac{1}{2}$. When $H < \frac{1}{2}$ we need to multiply by $T^{\frac{1}{2}-H}$ in order to obtain a finite limit.

The results of Theorem 1 can be used in order to derive approximation formulas for the price of European and Asian call options. Notice that

$$V_0^E = B_E(0, S_0, k, I_E(0, k)) \quad \text{and} \quad V_0^A = B_A(0, S_0, y_0, k, I_A(0, k)).$$

Then, using Taylor's formula we can use the approximations

$$\begin{aligned} I_E(0, k) &\approx I_E(0, k^*) + \partial_k I_E(0, k^*)(k - k^*), \\ I_A(0, k) &\approx I_A(0, k^*) + \partial_k I_A(0, k^*)(k - k^*). \end{aligned} \tag{9}$$

The great utility of these relations is that we can use them to approximate the price of European and Asian call options for a wide range of stochastic and fractional volatility models. We numerically investigate the quality of this approximation for the SABR and fractional Bergomi models in Section 5.3.

3 Preliminary results: decomposition formulas

In this section we provide closed form decomposition formulas for the prices and for the ATM implied volatility skew of European and Asian call options under the stochastic volatility model (1) that will be crucial for the proof of the main results.

We start with a preliminary lemma.

Lemma 1. *Consider the model (1). Let $0 \leq t \leq s \leq T$, $\rho \in (-1, 1)$ and $\mathcal{G}_t := \mathcal{F}_t \vee \mathcal{F}_T^{W'}$. Then for every $n \geq 0$, there exists $C = C(n, \rho)$ such that*

$$\begin{aligned} \left| \mathbb{E} \left(\frac{\partial^n}{\partial x^n} \left(\frac{\partial^2}{\partial x^2} B_E(s, M_s, k, v_s) \right) \middle| \mathcal{G}_t \right) \right| &= \left| \mathbb{E} \left(\frac{\partial^n}{\partial x^n} \left(\frac{\partial^2}{\partial x \partial k} B_E(s, M_s, k, v_s) \right) \middle| \mathcal{G}_t \right) \right| \\ &\leq C \left(\int_t^T \phi_r^2 dr \right)^{-\frac{n+1}{2}}, \end{aligned}$$

where $v_t = \sqrt{\frac{1}{T-t} \int_t^T \phi_r^2 dr}$

Proof. The proof follows the same steps as the proof of Lemma 6.3.1 in [2]. \square

The main result of this section is the following theorem.

Theorem 2. *Assume Hypotheses 1-3. Then, the following relations hold for all $t \in [0, T]$,*

$$\begin{aligned} V_t^E &= \mathbb{E}_t (B_E(t, S_t, k, v'_t)) + \mathbb{E}_t \left(\int_t^T H(s, S_s, k, v'_s) \sigma_s \left(\int_s^T D_s^W \sigma_r^2 dr \right) ds \right), \\ V_t^A &= \mathbb{E}_t (B_E(t, M_t, k, v_t)) + \mathbb{E}_t \left(\int_t^T H(s, M_s, k, v_s) \phi_s \left(\int_s^T D_s^W \phi_r^2 dr \right) ds \right), \end{aligned}$$

where $H(s, x, k, \sigma) = \frac{1}{2} \partial_{xxx}^3 B_E(s, x, k, \sigma)$, $v'_t = \sqrt{\frac{1}{T-t} \int_t^T \sigma_s^2 ds}$, and $v_t = \sqrt{\frac{1}{T-t} \int_t^T \phi_s^2 ds}$.

Proof. The proof follows similar ideas as the proof of Theorem 25 in [1]. See also Theorem 6.3.2 in [2]. Notice that, as $B_E(T, x, k, \sigma) = (x - k)_+$ for every $\sigma > 0$, the prices of our European and Asian call options can be written as

$$V_t^E = \mathbb{E}_t(B_E(T, S_T, k, v'_T)) \quad \text{and} \quad V_t^A = \mathbb{E}_t(B_E(T, M_T, k, v_T)).$$

We provide the proof of the decomposition formula for V_t^A . A similar argument applies for V_t^E and we safely skip it. Applying Theorem 3 to the function $B_E(t, M_t, k, v_t)$ and $Y_t = \int_t^T \phi_s^2 ds$ noticing that $v_t = \sqrt{\frac{Y_t}{T-t}}$, we obtain

$$\begin{aligned} B_E(T, M_T, k, v_T) &= B_E(t, M_t, k, v_t) \\ &+ \int_t^T \left(\partial_s B_E(s, M_s, k, v_s) + \partial_\sigma B_E(s, M_s, k, v_s) \frac{v_s^2}{2(T-s)v_s} \right) ds \\ &+ \int_t^T \partial_x B_E(s, M_s, k, v_s) \phi_s dW_s - \int_t^T \partial_\sigma B_E(s, M_s, k, v_s) \frac{\phi_s^2}{2(T-s)v_s} ds \\ &+ \int_t^T \partial_{xx}^2 B_E(s, M_s, k, v_s) \frac{\phi_s}{2(T-s)v_s} \left(\int_s^T D_s^W \phi_r^2 dr \right) ds \\ &+ \frac{1}{2} \int_t^T \partial_{xx}^2 B_E(s, M_s, k, v_s) \phi_s^2 ds. \end{aligned}$$

Notice that the following relation holds

$$\partial_{xx}^2 B_E(s, M_s, k, \sigma) = \frac{\partial_\sigma B_E(s, M_s, k, \sigma)}{\sigma(T-s)}. \quad (10)$$

Then we get the following

$$\begin{aligned} B_E(T, M_T, k, v_T) &= B_E(t, M_t, k, v_t) \\ &+ \int_t^T \left(\partial_s B_E(s, M_s, k, v_s) + \frac{1}{2} v_s^2 \partial_{xx}^2 B_E(s, M_s, k, v_s) \right) ds \\ &+ \int_t^T \partial_x B_E(s, M_s, k, v_s) \phi_s dW_s - \frac{1}{2} \int_t^T \partial_{xx}^2 B_E(s, M_s, k, v_s) \phi_s^2 ds \\ &+ \frac{1}{2} \int_t^T \partial_{xxx}^3 B_E(s, M_s, k, v_s) \phi_s \left(\int_s^T D_s^W \phi_r^2 dr \right) ds \\ &+ \frac{1}{2} \int_t^T \partial_{xx}^2 B_E(s, M_s, k, v_s) \phi_s^2 ds. \end{aligned}$$

The first integral in the above expression is equal to zero due to equation (5). Finally, taking conditional expectations we conclude that

$$\begin{aligned} \mathbb{E}_t(B_E(T, M_T, k, v_T)) &= \mathbb{E}_t(B_E(t, M_t, k, v_t)) \\ &+ \mathbb{E}_t \left(\frac{1}{2} \int_t^T \partial_{xxx}^3 B_E(s, M_s, k, v_s) \phi_s \left(\int_s^T D_s^W \phi_r^2 dr \right) ds \right). \end{aligned}$$

Observe that by Lemma 1 and Hypotheses 1 and 3(2), the last conditional expectation is finite. This completes the desired proof. \square

Based on the result of Theorem 2, we derive an expression for the ATMIV skew of European and Asian call options under the stochastic volatility model (1).

Proposition 1. Assume Hypotheses 1-3. Then, for every $t \in [0, T]$ the following holds

$$\begin{aligned}\partial_k I_E(t, k_t^*) &= \frac{\mathbb{E}_t \left(\int_t^T \partial_k H(s, S_s, k_t^*, v_s') \Lambda_s' ds \right)}{\partial_\sigma B_E(t, S_t, k_t^*, I_E(t, k_t^*))}, \\ \partial_k I_A(t, k_t^*) &= \frac{\mathbb{E}_t \left(\int_t^T \partial_k H(s, M_s, k_t^*, v_s) \Lambda_s ds \right)}{\partial_\sigma B_A(t, S_t, y_t, k_t^*, I_A(t, k_t^*))},\end{aligned}$$

where $\Lambda_s' = \sigma_s \int_s^T D_s^W \sigma_r^2 dr$ and $\Lambda_s = \phi_s \int_s^T D_s^W \phi_r^2 dr$.

Proof. We provide the proof for the second part of the theorem. The first part follows by similar arguments. Since $V_t^A = B_A(t, S_t, y_t, k, I_A(t, k))$, differentiating we obtain that

$$\partial_k V_t^A = \partial_k B_A(t, S_t, y_t, k, I_A(t, k)) + \partial_\sigma B_A(t, S_t, y_t, k, I_A(t, k)) \partial_k I_A(t, k).$$

On the other hand, using Theorem 2, we get that

$$\partial_k V_t^A = \partial_k \mathbb{E}_t (B_E(t, M_t, k, v_t)) + \mathbb{E}_t \left(\int_t^T \partial_k H(s, M_s, k, v_s) \Lambda_s ds \right).$$

Combining both equations, we obtain that the volatility skew $\partial_k I_A(t, k)$ is equal to

$$\frac{\mathbb{E}_t \left(\int_t^T \partial_k H(s, M_s, k, v_s) \Lambda_s ds \right) + \mathbb{E}_t (\partial_k B_E(t, M_t, k, v_t)) - \partial_k B_A(t, S_t, y_t, k, I_A(t, k))}{\partial_\sigma B_A(t, S_t, y_t, k, I_A(t, k))}.$$

Finally, using the fact that

$$\partial_k B_E(t, M_t, k_t^*, \sigma) = \partial_k B_A(t, S_t, y_t, k_t^*, \sigma) = -\frac{1}{2}$$

we complete the desired proof. \square

In order to compute the limit of ATMIV skew, we need to identify the leading order terms in the numerator of the formulas obtained in Proposition 1, for which the next result will be crucial.

Proposition 2. Assume Hypotheses 1-3. Then, for all $t \leq T$,

$$\begin{aligned}\mathbb{E}_t \left(\int_t^T G(s, S_s, k, v_s') \Lambda_s' ds \right) &= \mathbb{E}_t (G(t, S_t, k, v_t') J_t') \\ &\quad + \mathbb{E}_t \left(\frac{1}{2} \int_t^T \partial_{xxx}^3 G(s, S_s, k, v_s') J_s' \Lambda_s' ds \right) \\ &\quad + \mathbb{E}_t \left(\int_t^T \partial_x G(s, S_s, k, v_s') \sigma_s D^- J_s' ds \right), \\ \mathbb{E}_t \left(\int_t^T G(s, M_s, k, v_s) \Lambda_s ds \right) &= \mathbb{E}_t (G(t, M_t, k, v_t) J_t) \\ &\quad + \mathbb{E}_t \left(\frac{1}{2} \int_t^T \partial_{xxx}^3 G(s, M_s, k, v_s) J_s \Lambda_s ds \right) \\ &\quad + \mathbb{E}_t \left(\int_t^T \partial_x G(s, M_s, k, v_s) \phi_s D^- J_s ds \right),\end{aligned}$$

where $G(t, x, k, \sigma) = \partial_k H(t, x, k, \sigma)$, $J_t = \int_t^T \Lambda_s ds$, $J_t' = \int_t^T \Lambda_s' ds$, $D^- J_s' = \int_s^T D_s^W \Lambda_r' dr$ and $D^- J_s = \int_s^T D_s^W \Lambda_r dr$.

Proof. We only prove the second part of the theorem since the first part follows by similar arguments. Applying Theorem 3 to the function $\partial_k H(t, M_t, k, v_t) \int_t^T \Lambda_s ds$, we obtain that

$$\begin{aligned} \int_t^T G(s, M_s, k, v_s) \Lambda_s ds &= G(t, M_t, k, v_t) J_t \\ &+ \int_t^T \left(\partial_s G(s, M_s, k, v_s) + \frac{v_s^2}{2(T-s)v_s} \partial_v G(s, M_s, k, v_s) \right) J_s ds \\ &+ \int_t^T \partial_x G(s, M_s, k, v_s) J_s \phi_s dW_s \\ &- \int_t^T \partial_v G(s, M_s, k, v_s) J_s \frac{\phi_s^2}{2(T-s)v_s} ds + \int_t^T \partial_{vx}^2 G(s, M_s, k, v_s) J_s \Lambda_s \frac{1}{2(T-s)v_s} ds \\ &+ \int_t^T \partial_x G(s, M_s, k, v_s) \phi_s D^- J_s ds + \frac{1}{2} \int_t^T \phi_s^2 \partial_{xx}^2 G(s, M_s, k, v_s) J_s ds. \end{aligned}$$

Next, equations (5) and (10) imply that

$$\begin{aligned} \partial_s G(s, M_s, k, v_s) + \frac{1}{2} v_s^2 \partial_{xx}^2 G(s, M_s, k, v_s) &= 0, \\ \partial_{xx}^2 G(s, M_s, k, v_s) &= \frac{\partial_v G(s, M_s, k, v_s)}{v_s(T-s)}. \end{aligned}$$

Using the above equations we get that

$$\begin{aligned} \int_t^T G(s, M_s, k, v_s) \Lambda_s ds &= G(t, M_t, k, v_t) J_t + \int_t^T \partial_x G(s, M_s, k, v_s) J_s \phi_s dW_s \\ &+ \frac{1}{2} \int_t^T \partial_{xxx}^3 G(s, M_s, k, v_s) J_s \Lambda_s ds + \int_t^T \partial_x G(s, M_s, k, v_s) \phi_s D^- J_s ds. \end{aligned}$$

Finally, taking conditional expectations and noticing that by Lemma 1 and Hypotheses 1 and 3, all conditional expectations are finite, we complete the desired proof. \square

4 Proof of Theorem 1

4.1 Proof of (6) in Theorem 1: ATM implied volatility level

This section is devoted to the proof of (6) in Theorem 1. We only show the result for $I_A(0, k^*)$ since the proof for $I_E(0, k^*)$ follows along the same lines. We start proving the result for the implied volatility in the uncorrelated case ($\rho = 0$) that we denote by $I_A^0(t, k)$.

4.1.1 The uncorrelated case

We aim to apply the decomposition for the option price obtained in Theorem 2. Observe that

$$D_s^W \phi_r^2 dr = \frac{(T-r)^2}{T^2} D_s^W \sigma_r^2 = \frac{(T-r)^2}{T^2} 2\sigma_r D_s^W \sigma_r = \frac{(T-r)^2}{T^2} 2\sigma_r \rho D_s^{W'} \sigma_r.$$

Thus, if $\rho = 0$, the decomposition formula give us that $V_0^A = \mathbb{E}(B_E(0, M_0, k, v_0))$. Then the ATMIV satisfies that

$$\begin{aligned} I_A^0(0, k^*) &= (B_A)^{-1}(0, S_0, y_0, k^*, V_0^A) = \mathbb{E}(B_A^{-1}(0, S_0, y_0, k^*, \mathbb{E}B_E(0, M_0, k^*, v_0))) \\ &= \mathbb{E}(B_A^{-1}(0, S_0, y_0, k^*, \mathbb{E}B_E(0, M_0, k^*, v_0)) \pm B_A^{-1}(0, S_0, y_0, k^*, B_E(0, M_0, k^*, v_0))) \\ &= \mathbb{E}(B_A^{-1}(0, S_0, y_0, k^*, \Phi_0) - B_A^{-1}(0, S_0, y_0, k^*, \Phi_T)) + \sqrt{3}\mathbb{E}(v_0) \\ &= \sqrt{3}\mathbb{E}(B_E^{-1}(0, M_0, k^*, \Phi_0) - B_E^{-1}(0, M_0, k^*, \Phi_T)) + \sqrt{3}\mathbb{E}(v_0), \end{aligned}$$

where $\Phi_r := \mathbb{E}_r(B_E(0, M_0, k^*, v_0))$. The last two lines follow from the observation that $B_A^{-1}(t, S_t, y_t, k_t^*, B_E(t, M_t, k_t^*, \sigma)) = \frac{T\sqrt{3}}{T-t}\sigma$.

Observe that as $\rho = 0$, the Brownian motions W and W' are independent. Thus, $\Phi_r = \mathbb{E}(B_E(0, M_0, k^*, v_0) | \mathcal{F}_r^{W'})$ and $(\Phi_r)_{r \geq 0}$ is a martingale wrt to the filtration $(\mathcal{F}_r^{W'})_{r \geq 0}$. By the martingale representation theorem, there exists a square integrable and $\mathcal{F}^{W'}$ -adapted process $(U_r)_{r \geq 0}$ such that

$$\Phi_r = \Phi_0 + \int_0^r U_s dW'_s.$$

A direct application of the classical Itô's formula gives

$$\begin{aligned} & \mathbb{E}(B_E^{-1}(0, M_0, k^*, \Phi_0) - B_E^{-1}(0, M_0, k^*, \Phi_T)) \\ &= -\mathbb{E}\left(\int_0^T (B_E^{-1})'(0, M_0, k^*, \Phi_s) U_s dW'_s + \frac{1}{2} \int_0^T (B_E^{-1})''(0, M_0, k^*, \Phi_s) U_s^2 ds\right), \end{aligned}$$

where $(B_E^{-1})'$ and $(B_E^{-1})''$ denote, respectively, the first and second derivative of B_E^{-1} with respect to σ . A direct computation gives

$$B_E^{-1}(0, M_0, k^*, \Phi_s) = \frac{\Phi_s \sqrt{2\pi}}{\sqrt{T}} \quad \text{and} \quad ((B_E)^{-1})''(0, M_0, k^*, \Phi_s) = 0,$$

which leads to

$$I_A^0(0, k^*) = \sqrt{3}\mathbb{E}(v_0).$$

By continuity, we conclude that

$$\lim_{T \rightarrow 0} I_A^0(0, k^*) = \sigma_0, \tag{11}$$

which proves (6) in the uncorrelated case.

4.1.2 The correlated case

Using similar ideas as in the uncorrelated case we get that

$$\begin{aligned} I_A(0, k^*) &= (B_A)^{-1}(0, S_0, y_0, k^*, V_0^A) \\ &= \mathbb{E}((B_A)^{-1}(0, S_0, y_0, k^*, \Gamma_T) \pm (B_A)^{-1}(0, S_0, y_0, k^*, \Gamma_0)) \\ &= \mathbb{E}((B_A)^{-1}(0, S_0, y_0, k^*, \Gamma_T) - (B_A)^{-1}(0, S_0, y_0, k^*, \Gamma_0)) + I_A^0(0, k^*) \\ &= \sqrt{3}\mathbb{E}(B_E^{-1}(0, M_0, k^*, \Gamma_T) - B_E^{-1}(0, M_0, k^*, \Gamma_0)) + I_A^0(0, k^*), \end{aligned}$$

where $\Gamma_s := \mathbb{E}[B_E(0, M_0, k^*, v_0)] + \frac{\rho}{2}\mathbb{E}(\int_0^s H(r, M_r, k_r^*, v_r) \Lambda_r dr)$.

A direct application of Itô's formula gives

$$\begin{aligned} I_A(0, k^*) &= I_A^0(0, k^*) + \mathbb{E}\left(\int_0^T (B_E^{-1})'(0, M_0, k^*, \Gamma_s) H(s, M_s, k_s^*, v_s) \Lambda_s ds\right) \\ &= I_A^0(0, k^*) + \frac{\sqrt{2\pi}}{\sqrt{T}} \mathbb{E}\left(\int_0^T H(s, M_s, k_s^*, v_s) \Lambda_s ds\right). \end{aligned}$$

Next, Hypotheses 1 and 3 together with Lemma 1 imply that

$$\begin{aligned} & \left| \mathbb{E}\left(\int_0^T H(s, M_s, k^*, v_s) \Lambda_s ds\right) \right| \leq C \mathbb{E}\left(\left(\int_0^T \phi_r^2 dr\right)^{-1} \left(\int_0^T |\Lambda_s| ds\right)\right) \\ & \leq C \left(\int_0^T \frac{(T-r)^2}{T^2} dr\right)^{-1} \int_0^T \frac{(T-s)^3}{T^3} \int_s^T \mathbb{E}(|D_s^{W'} \sigma_r|) dr ds \\ & \leq C \frac{1}{T^4} \int_0^T (T-s)^3 \int_s^T (r-s)^{H-\frac{1}{2}} dr ds \\ & = CT^{H+\frac{1}{2}}. \end{aligned}$$

Thus, we conclude that $\frac{1}{\sqrt{T}} \mathbb{E} \left(\int_0^T H(s, M_s, k_t^*, v_s) \Lambda_s ds \right) \rightarrow 0$ as $T \rightarrow 0$. Finally, using (11), we get that

$$I_A(0, k^*) \rightarrow \sigma_0$$

as $T \rightarrow 0$, which concludes the proof of (6).

4.2 Proof of (7) in Theorem 1: ATMIV skew

We provide the proof for the Asian call option case. The result for the European call follows by the same argument.

Appealing to Propositions 1 and 2 we have that

$$\begin{aligned} \partial_k I_A(0, k^*) &= \frac{1}{\partial_\sigma B_A(0, S_0, y_0, k^*, I_A(0, k^*))} \left\{ \mathbb{E} (G(0, M_0, k^*, v_0) J_0) \right. \\ &\quad + \mathbb{E} \left(\frac{1}{2} \int_0^T \partial_{xxx}^3 G(s, M_s, k^*, v_s) J_s \Lambda_s ds \right) \\ &\quad \left. + \mathbb{E} \left(\int_0^T \partial_x G(s, M_s, k^*, v_s) \phi_s D^- J_s ds \right) \right\}. \end{aligned} \quad (12)$$

We start bounding the second term in (12). Using Hypotheses 1 and 3 together with Cauchy-Schwarz inequality we get that

$$\begin{aligned} &\mathbb{E}(|J_s \Lambda_s|) \\ &\leq C \frac{(T-s)}{T^6} \mathbb{E} \left(\left(\int_s^T (T-r)^2 |D_s^{W'} \sigma_r| dr \right) \left(\int_s^T (T-u)^3 \int_u^T |D_u^{W'} \sigma_r| dr du \right) \right) \\ &\leq C \frac{(T-s)}{T^6} \sqrt{\mathbb{E} \left(\left(\int_s^T (T-r)^2 |D_s^{W'} \sigma_r| dr \right)^2 \right) \mathbb{E} \left(\left(\int_s^T (T-u)^3 \int_u^T |D_u^{W'} \sigma_r| dr du \right)^2 \right)} \\ &\leq C \frac{(T-s)}{T^6} \sqrt{(T-s)^5 \int_s^T \mathbb{E}(|D_s^{W'} \sigma_r|^2) dr} (T-s)^8 \int_s^T \int_u^T \mathbb{E}(|D_u^{W'} \sigma_r|^2) dr du \\ &\leq C \frac{(T-s)^{2H+8}}{T^6}. \end{aligned}$$

Then, using Lemma 1 we conclude that

$$\begin{aligned} &\left| \mathbb{E} \left(\frac{1}{2} \int_0^T \partial_{xxx}^3 G(s, M_s, k, v_s) J_s \Lambda_s ds \right) \right| \\ &\leq C \frac{1}{T^3} \int_0^T \frac{(T-s)^{2H+8}}{T^6} dt = CT^{2H}. \end{aligned}$$

We next bound the third term in (12). We have that

$$\begin{aligned} \int_s^T D_s^W \Lambda_r dr &= \int_s^T D_s^W \left(\phi_r \int_r^T D_r^W \phi_u^2 du \right) dr \\ &= \int_s^T \left((D_s^W \phi_r) \int_r^T D_r^W \phi_u^2 du + \phi_r \int_r^T D_s^W D_r^W \phi_u^2 du \right) dr, \end{aligned}$$

where

$$D_s^W D_r^W \phi_u^2 = 2(D_s^W \phi_u D_r^W \phi_u + \phi_u D_s^W D_r^W \phi_u).$$

Hypothesis 1 implies that

$$|D_s^W D_r^W \phi_u^2| \leq C \frac{(T-u)^2}{T^2} \left(|D_s^{W'} \sigma_u| |D_r^{W'} \sigma_u| + |D_s^{W'} D_r^{W'} \sigma_u| \right).$$

Then, appealing to Hypothesis 3, we get that

$$\begin{aligned}\mathbb{E} \left(\left| \phi_r \int_r^T D_s^W D_r^W \phi_u^2 du \right| \right) &\leq C \frac{(T-r)^3}{T^3} \int_r^T (u-r)^{H-\frac{1}{2}} (u-s)^{H-\frac{1}{2}} du \\ &\leq C \frac{(T-r)^3}{T^3} (T-s)^{2H}\end{aligned}$$

and

$$\begin{aligned}\mathbb{E} \left(\left| D_s^W \phi_r \int_r^T D_r^W \phi_u^2 du \right| \right) &\leq C \frac{(T-r)^3}{T^3} \mathbb{E} \left(|D_s^{W'} \sigma_r| \int_r^T |D_r^{W'} \sigma_u| du \right) \\ &\leq C \frac{(T-r)^3}{T^3} (r-s)^{H-\frac{1}{2}} (T-r)^{H+\frac{1}{2}}.\end{aligned}$$

Therefore, we conclude that

$$\begin{aligned}\mathbb{E} \left(\left| \int_s^T D_s^W \Lambda_r dr \right| \right) &\leq C \int_s^T \frac{(T-r)^3}{T^3} \left((r-s)^{H-\frac{1}{2}} (T-s)^{H+\frac{1}{2}} + (T-s)^{2H} \right) dr \\ &\leq C \frac{(T-s)^{2H+4}}{T^3}.\end{aligned}$$

Finally, using Lemma 1 we obtain that the third term in (12) satisfies that

$$\begin{aligned}\left| \mathbb{E} \left(\int_0^T \partial_x G(s, M_s, k, v_s) \phi_s D^- J_s ds \right) \right| &\leq C \frac{1}{T^2} \int_0^T \frac{(T-s)^{5+2H}}{T^4} ds \\ &= CT^{2H}.\end{aligned}$$

Taking into account the relation $\partial_\sigma B_A(0, S_0, y_0, k^*, \sigma) = \frac{1}{\sqrt{3}} \partial_\sigma B_E(0, S_0, k^*, \sigma)$ we get that

$$\partial_\sigma B_A(0, S_0, y_0, k^*, \sigma) = \frac{\sqrt{T}}{\sqrt{6\pi}}.$$

Thus, as

$$\lim_{T \rightarrow 0} T^{\max(\frac{1}{2}-H, 0)} \frac{1}{\sqrt{T}} T^{2H} = 0,$$

the second and third terms in (12) will contribute as 0 in the limit (8).

We finally study the first term in (12). Direct differentiation give us that

$$G(0, M_0, k^*, v_0) = \frac{1}{2\sqrt{2\pi} v_0^3 T^{3/2}}.$$

Thus, by (12), we get that

$$\begin{aligned}\lim_{T \rightarrow 0} T^{\max(\frac{1}{2}-H, 0)} \partial_k I_A(0, k^*) \\ = \sqrt{3} \rho \lim_{T \rightarrow 0} T^{\max(\frac{1}{2}-H, 0)} \frac{1}{T^5} \mathbb{E} \left(v_0^{-3} \int_0^T \sigma_r (T-r) \int_r^T \sigma_u (T-u)^2 D_r^{W'} \sigma_u du dr \right).\end{aligned}$$

By continuity, it holds that v_0^{-3} converges towards $\sigma_0^{-3} \sqrt{3}^3$ a.s. as $T \rightarrow 0$. On the other hand, by Hypotheses 1 and (2), we have that

$$\begin{aligned}\left| \mathbb{E} \left(\int_0^T \sigma_r (T-r) \int_r^T \sigma_u (T-u)^2 D_r^{W'} \sigma_u du dr \right) \right| \\ \leq C \int_0^T (T-r)^3 \int_r^T (u-r)^{H-\frac{1}{2}} du dr \\ \leq CT^{4+H+\frac{1}{2}}.\end{aligned}$$

Thus, by dominated convergence, we conclude the proof of (8).

5 Numerical analysis

In this section we apply the theoretical results presented earlier to some examples of stochastic volatility models. We justify our findings with numerical simulations.

5.1 The SABR model

We consider the SABR stochastic volatility model with skewness parameter 1, which is the most common case from a practical point of view. This corresponds to equation (1), where S_t denotes the forward price of the underlying asset and

$$d\sigma_t = \alpha \sigma_t dW'_t, \quad \sigma_t = \sigma_0 e^{\alpha W'_t - \frac{\alpha^2}{2} t}.$$

where $\alpha > 0$ is the volatility of volatility.

Notice that this model does not satisfy Hypothesis 1, so a truncation argument is needed in order to check that Theorem 1 is true for this model. We skip it here for the sake of simplicity since it is identical to the one presented in Alós, Nualart, Pravosud [5].

For $r \leq t$, we have that $D_r^{W'} \sigma_t = \alpha \sigma_t$ and $\mathbb{E}(D_r^{W'} \sigma_t) = \alpha \sigma_0$. Therefore, applying Theorem 1 we conclude that

$$\begin{aligned} \lim_{T \rightarrow 0} \partial_k I_A(0, k^*) &= \frac{3}{5} \rho \alpha, \\ \lim_{T \rightarrow 0} \partial_k I_E(0, k^*) &= \frac{1}{2} \rho \alpha. \end{aligned}$$

We next proceed with some numerical simulations using the following parameters

$$S_0 = 10, T = \frac{1}{252}, dt = \frac{T}{50}, \alpha = 0.5, \rho = -0.3, \sigma_0 = (0.1, 0.2, \dots, 1.4).$$

In order to get estimates of an Asian call option we use antithetic variates. The estimator of the price is defined as follows

$$\hat{V}_{sabr} = \frac{\frac{1}{N} \sum_{i=1}^N V_T^i + \frac{1}{N} \sum_{i=1}^N V_T^{i,A}}{2}, \quad (13)$$

where $N = 2000000$ and the sub-index A denotes the value of an Asian call option computed on the antithetic trajectory of a Monte Carlo path.

In order to retrieve the implied volatility we use method presented in Jaeckel [13]. For the estimation of the skew, we use the following expression which allows us to avoid a finite difference method

$$\begin{aligned} \partial_k \hat{I}^A(0, k^*) &= \frac{-\partial_k B_A(0, X_0, y_0, k^*, I_A(0, k^*)) - \mathbb{E}(1_{A_T \geq k^*})}{\partial_\sigma B_A(0, X_0, y_0, k^*, I_A(0, k^*))} = \frac{\frac{1}{2} - \mathbb{E}(1_{A_T \geq k^*})}{\sqrt{\frac{T}{6\pi}}}, \\ \partial_k \hat{I}^E(0, k^*) &= \frac{-\partial_k B_E(0, S_0, k^*, I_E(0, k^*)) - \mathbb{E}(1_{S_T \geq k^*})}{\partial_\sigma B_E(0, S_0, k^*, I_E(0, k^*))} = \frac{\frac{1}{2} - \mathbb{E}(1_{S_T \geq k^*})}{\sqrt{\frac{T}{2\pi}}}. \end{aligned} \quad (14)$$

We use equation (14) in order to get estimates of the skew. In Figure 1 we present the results of a Monte Carlo simulation which aims to evaluate numerically the level and the skew of the at-the-money implied volatility of an Asian call option under the SABR model. And in Figure 2 we do the same, but for the European call option. We observe that all the numerical results fit the theoretical ones.

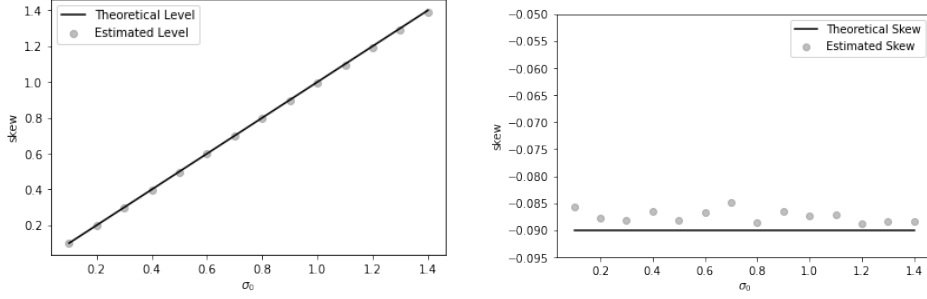


Figure 1: At-the-money level and the skew of the Implied Volatility of an Asian call under the SABR model.

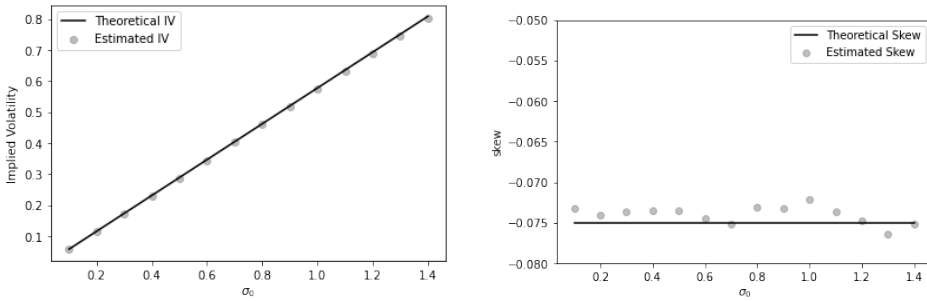


Figure 2: At-the-money level and the skew of the Implied Volatility of the European call option under the SABR model.

5.2 The fractional Bergomi model

The fractional Bergomi stochastic volatility model assumes equation (1) with

$$\sigma_t^2 = \sigma_0^2 e^{v\sqrt{2H}Z_t - \frac{1}{2}v^2t^{2H}},$$

$$Z_t = \int_0^t (t-s)^{H-\frac{1}{2}} dW_s,$$

where $H \in (0, 1)$ and $v > 0$.

As for the SABR model, a truncation argument as in Alós, Nualart, Pravosud [5] is needed in order to apply the results in the previous sections, as Hypothesis 1 is not satisfied. Moreover, for $r \leq u$, we have

$$D_r^{W'} \sigma_u = \frac{1}{2} \sigma_u v \sqrt{2H} (u-r)^{H-\frac{1}{2}},$$

$$\mathbb{E}(D_r^{W'} \sigma_u) = e^{-\frac{1}{8}v^2u^{2H}} \frac{1}{2} \sigma_0 v \sqrt{2H} (u-r)^{H-\frac{1}{2}},$$

which gives

$$\lim_{T \rightarrow 0} \partial_k I_A(0, k^*) = \begin{cases} 0 & \text{if } H > \frac{1}{2}, \\ \frac{3\rho v}{10} & \text{if } H = \frac{1}{2}, \end{cases}, \quad (15)$$

$$\lim_{T \rightarrow 0} \partial_k I_E(0, k^*) = \begin{cases} 0 & \text{if } H > \frac{1}{2}, \\ \frac{\rho v}{4} & \text{if } H = \frac{1}{2}. \end{cases}$$

and for $H < \frac{1}{2}$

$$\begin{aligned}\lim_{T \rightarrow 0} T^{\frac{1}{2}-H} \partial_k I_A(0, k^*) &= \frac{288\rho v \sqrt{2H}}{(2H+9)(8H^3+36H^2+46H+15)}, \\ \lim_{T \rightarrow 0} T^{\frac{1}{2}-H} \partial_k I_E(0, k^*) &= \frac{2\rho v \sqrt{2H}}{(3+4H(2+H))}.\end{aligned}\quad (16)$$

The parameters used for the Monte Carlo simulation are the following

$$S_0 = 100, T = 0.001, dt = \frac{T}{50}, H = (0.4, 0.7), v = 0.5, \rho = -0.3, \sigma_0 = (0.1, 0.2, \dots, 1.4).$$

In order to get estimates of the price of an Asian call option under the fractional Bergomi model we use antithetic variates presented in equation (13). Then, the level of at-the-money implied volatility of an Asian and European call options are presented on Figures 3 and 4, respectively. One can see that the result is independent of H .

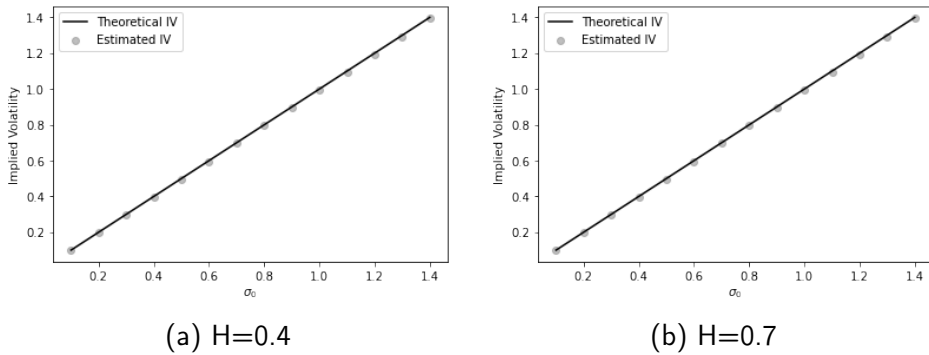


Figure 3: At-the-money level of the IV of an Asian call under fractional Bergomi model.

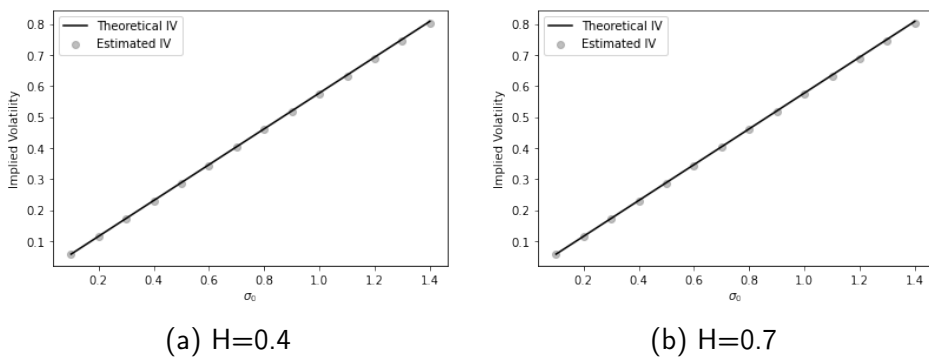


Figure 4: At-the-money level of the IV of the European call under fractional Bergomi model.

On Figures 5 and 6 we present the ATM implied volatility skew as a function of maturity of an Asian and European call options, respectively, for two different values of H , where we observe the blow up to $-\infty$ for the case $H = 0.4$. Equation (15) suggests that the theoretical values of the slope of the at-the-money skew (as a function αT^β) in the cases of Asian and European call options with $H < \frac{1}{2}$ are -0.0497 and -0.0336 , respectively. We conclude that theoretical results are in line with the observed numbers. Due to the blow up of the

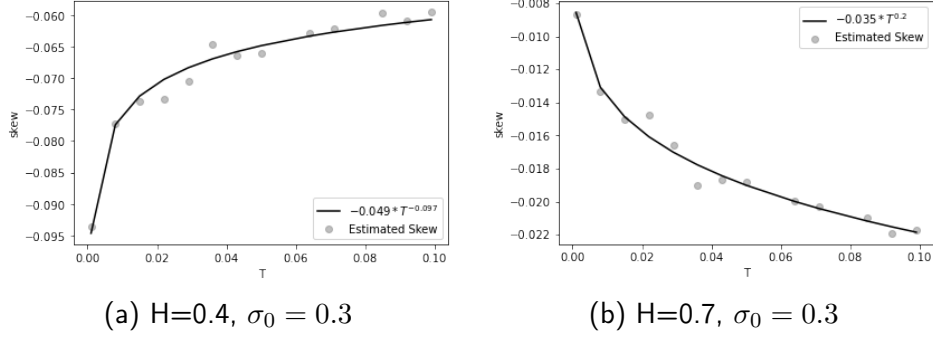


Figure 5: At-the-money IV skew of an Asian call as a function of T under fractional Bergomi model.

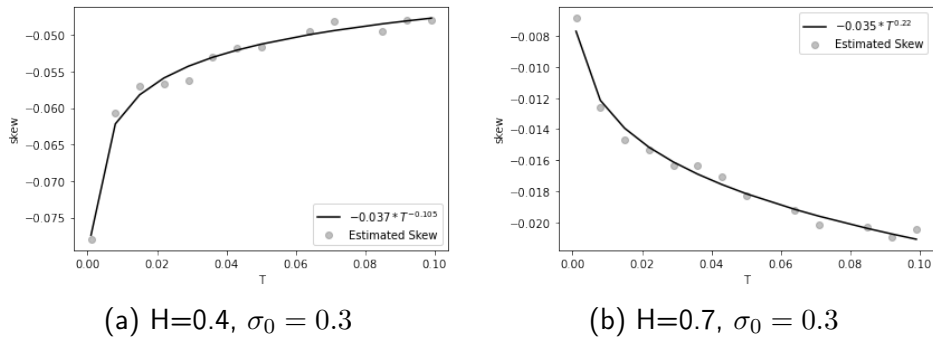


Figure 6: At-the-money IV skew of the European call as a function of T under fractional Bergomi model.

at-the-money implied volatility skew of an Asian and European call options when $H < \frac{1}{2}$ we also plot (as a function of σ_0) the quantities $T^{\frac{1}{2}-H} \partial_k \hat{I}^A(0, k^*)$ and $T^{\frac{1}{2}-H} \partial_k \hat{I}^E(0, k^*)$ for $H = 0.4$ as well as $\partial_k \hat{I}^A(0, k^*)$ and $\partial_k \hat{I}^E(0, k^*)$ for $H = 0.7$ for fixed value of $T = 0.001$. The result is presented at Figures 7 and 8. We see that numerical estimates agree with the presented theoretical findings.

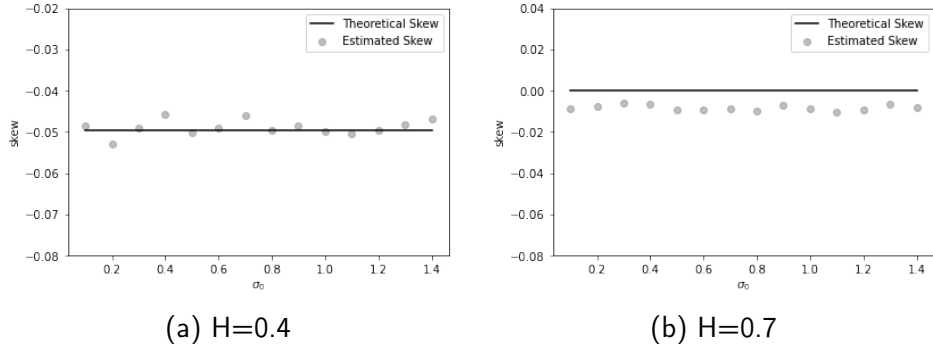


Figure 7: At-the-money IV skew of an Asian call as a function of σ_0 under fractional Bergomi model

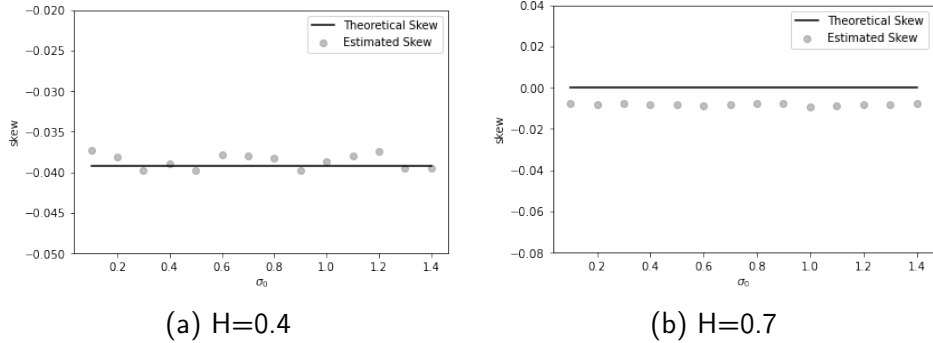


Figure 8: At-the-money IV skew of the European call as a function of σ_0 under fractional Bergomi model

5.2.1 Local volatility model

We consider the local volatility model

$$dS_t = \sigma(S_t)dW_t,$$

where $\sigma \in C_b^2$ (bounded with bounded first and second derivatives) and $\sigma(x) \geq c > 0$, for all x . We apply Theorem 1 when S_t follows this model with $\rho = 0$ and $\sigma_t = \sigma(S_t)$. Under the above assumptions it is easy to see that all the hypotheses are satisfied with $H = \frac{1}{2}$. Thus, for the ATMIV level, we directly see that the limit is equal to $\sigma(S_0)$. For the ATMIV skew, we need to compute $D_r\sigma(S_t)$. We have for $r \leq u$,

$$D_r^W \sigma(S_u) = \sigma'(S_u) D_r^W S_u = \sigma'(S_u) \left(\sigma(S_r) + \int_r^u D_r^W \sigma(S_s) dW_s \right).$$

In particular,

$$\mathbb{E}(D_r \sigma(S_u)) = \mathbb{E}(\sigma'(S_u) \sigma(S_r)) .$$

This can be written as

$$\begin{aligned}\mathbb{E}(D_r \sigma(S_u)) &= \sigma'(S_0) \sigma(S_0) + \mathbb{E}((\sigma'(S_u) - \sigma'(S_0)) \sigma(S_r)) \\ &\quad + \sigma'(S_0) \mathbb{E}((\sigma(S_r) - \sigma(S_0))).\end{aligned}$$

Then, using the mean value theorem and the fact that S_t has Hölder continuous sample paths of any order $\gamma < \frac{1}{2}$, we see that the last two terms of the last display will not contribute in the limit (7) and (8). Thus, we get

$$\lim_{T \rightarrow 0} \partial_k I_A(0, k^*) = \frac{3}{5} \sigma'(S_0),$$

$$\lim_{T \rightarrow 0} \partial_k I_E(0, k^*) = \frac{1}{2} \sigma'(S_0).$$

5.3 Approximations of implied volatility

In this last section we study numerically the adequacy of the linear approximation of the implied volatility of an Asian and European call options given by equation (9) in the case of the SABR and fractional Bergomi models.

5.3.1 Asian call option

We start our analysis by presenting the results for the case of an Asian call option.

The SABR Model We proceed with the following numerical experiment. We randomly sample the parameters as $\sigma_0 \sim U(0.2, 0.8)$, $\alpha \sim U(0.3, 1.5)$ and $\rho \sim U(-0.9, 0.9)$, where U stands for the uniform distribution. We fix $S_0 = 10$ and consider the following strikes

$$K = (9.97, 9.9743, 9.9786, 9.9829, 9.9872, 9.9915, 9.9958, 10.0001)$$

and maturities $T = (0.01, 0.1, 0.5, 1, 2)$. We consider the narrow OTM range around ATM region because due to the law of large numbers deep OTM quickly loose the value and prices become indistinguishable from 0. An Asian call option is priced using Monte Carlo with 100000 paths and discretization step 0.01 and the IV is estimated using the same approach as discussed in Section 5.1. The approximation accuracy of the Monte Carlo for the IV is computed using the pointwise relative error with respect to the 95% Monte Carlo confidence interval and is presented in Table 1.

| Maturity/Strike | 9.9700 | 9.9743 | 9.9786 | 9.9829 | 9.9872 | 9.9915 | 9.9958 | 10.0 |
|-----------------|--------|--------|--------|--------|--------|--------|--------|------|
| 0.01 | 0.94 | 0.92 | 0.91 | 0.91 | 0.91 | 0.92 | 0.93 | 0.94 |
| 0.1 | 0.94 | 0.94 | 0.94 | 0.95 | 0.95 | 0.95 | 0.95 | 0.95 |
| 0.50 | 1.02 | 1.02 | 1.02 | 1.02 | 1.02 | 1.0 | 1.0 | |
| 1.0 | 1.1 | 1.1 | 1.10 | 1.1 | 1.1 | 1.1 | 1.1 | 1.0 |
| 2.0 | 1.3 | 1.3 | 1.3 | 1.3 | 1.3 | 1.3 | 1.3 | 1.3 |

Table 1: Median percentage error wrt the 95% Monte Carlo confidence interval for an Asian call IV under the SABR model.

We then compare the estimated IV with the approximation formula (9). We compute in Table 2 the median relative percentage error, the 90% quantile and the maximum of the relative percentage error of the Monte Carlo prices computed across 2000 random parameter combinations. We consider the 90% quantile in order to take into account the fact that we might generate 'bad' parameter combinations that may require more Monte Carlo samples to converge. In order to help the visualization of these quantities we also plot the heat map in Figure 9.

Overall, we can see that the suggested implied volatility approximation performs well in the ATM region for short dated options. We achieve implied volatility approximation accuracy comparable to the original Monte Carlo simulation. However, the quality of it impairs as soon as we move in the maturity ($T > 0.5$) and moneyness dimension.

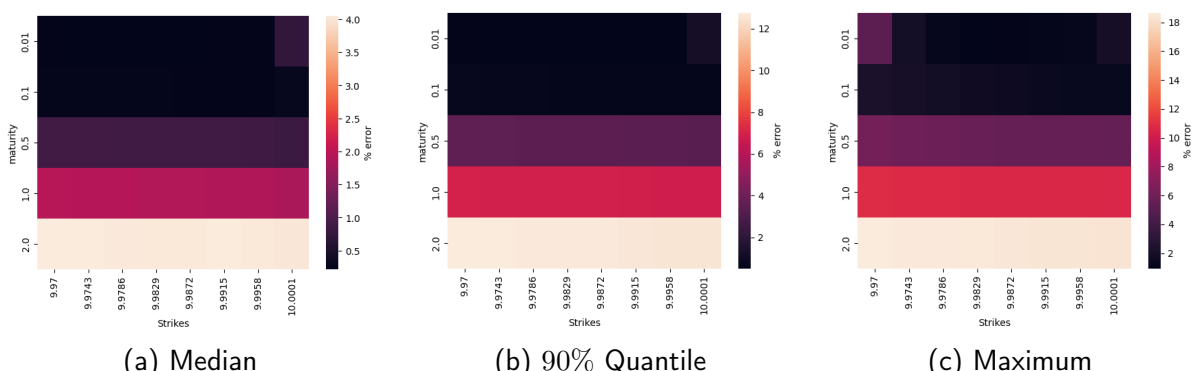


Figure 9: Accuracy of the approximation (9) for an Asian call under the SABR model.

| Maturity/Strike | 9.9700 | 9.9743 | 9.9786 | 9.9829 | 9.9872 | 9.9915 | 9.9958 | 10.0001 |
|-----------------|--------|--------|--------|--------|--------|--------|--------|---------|
| 0.01 | 0.24 | 0.23 | 0.22 | 0.23 | 0.23 | 0.24 | 0.24 | 0.72 |
| 0.10 | 0.26 | 0.25 | 0.25 | 0.25 | 0.24 | 0.24 | 0.24 | 0.29 |
| 0.50 | 0.89 | 0.89 | 0.87 | 0.87 | 0.87 | 0.87 | 0.86 | 0.81 |
| 1.00 | 1.95 | 1.93 | 1.92 | 1.91 | 1.90 | 1.89 | 1.89 | 1.84 |
| 2.00 | 4.04 | 4.04 | 4.03 | 4.01 | 4.02 | 4.05 | 4.02 | 4.00 |

(a) Median % error

| Maturity/Strike | 9.9700 | 9.9743 | 9.9786 | 9.9829 | 9.9872 | 9.9915 | 9.9958 | 10.0001 |
|-----------------|--------|--------|--------|--------|--------|--------|--------|---------|
| 0.01 | 0.57 | 0.54 | 0.51 | 0.51 | 0.51 | 0.53 | 0.53 | 1.18 |
| 0.10 | 0.71 | 0.69 | 0.66 | 0.64 | 0.63 | 0.62 | 0.61 | 0.63 |
| 0.50 | 3.53 | 3.50 | 3.47 | 3.45 | 3.44 | 3.41 | 3.41 | 3.36 |
| 1.00 | 6.94 | 6.92 | 6.91 | 6.90 | 6.90 | 6.86 | 6.82 | 6.79 |
| 2.00 | 12.76 | 12.75 | 12.71 | 12.67 | 12.67 | 12.58 | 12.55 | 12.54 |

(b) 90th quantile % Error

| Maturity/Strike | 9.9700 | 9.9743 | 9.9786 | 9.9829 | 9.9872 | 9.9915 | 9.9958 | 10.0001 |
|-----------------|--------|--------|--------|--------|--------|--------|--------|---------|
| 0.01 | 5.17 | 1.87 | 1.19 | 0.95 | 1.07 | 1.13 | 1.20 | 1.93 |
| 0.10 | 2.26 | 2.04 | 1.84 | 1.67 | 1.53 | 1.42 | 1.36 | 1.35 |
| 0.50 | 6.17 | 5.94 | 5.80 | 5.68 | 5.64 | 5.62 | 5.61 | 5.56 |
| 1.00 | 10.78 | 10.66 | 10.63 | 10.61 | 10.60 | 10.59 | 10.58 | 10.55 |
| 2.00 | 18.65 | 18.58 | 18.52 | 18.46 | 18.40 | 18.36 | 18.31 | 18.25 |

(c) Maximum % error

Table 2: Approximation error of Asian call IV under the SABR model.

In order to explain why the approximation impairs with the maturity of an option, we show a "typical" implied volatility surface in the simulated data set at Figure 10. One can see that ATM level of the implied volatility $I_A(0, k^*)$ changes considerably with the increase of maturity leading to the decrease in the quality of the linear approximation.

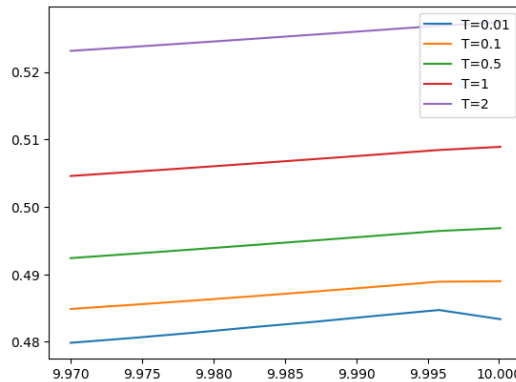


Figure 10: Typical surface of the IV of an Asian call under the SABR model.

fractional Bergomi Model In the case of the fractional Bergomi model we randomly sample the parameters of the model as $\sigma_0 \sim U(0.2, 0.8)$, $v \sim U(0.3, 1.5)$ and $\rho \sim U(-0.9, 0.9)$. We keep the values of S_0 , K and T identical to the one in the SABR case. In order to

investigate the influence of fractionalness of the volatility process we consider two values of $H = \{0.2, 0.7\}$. We price the Asian call option using Monte Carlo with 100000 paths and discretization step 0.01.

We start with the case $H = 0.2$. The implied volatility approximation accuracy using Monte Carlo is computed using the corresponding pointwise median relative error with respect to the 95% Monte Carlo confidence interval. The result is presented at Table 3. Next, we look

| Maturity/Strike | 9.9700 | 9.9743 | 9.9786 | 9.9829 | 9.9872 | 9.9915 | 9.9958 | 10.0001 |
|-----------------|--------|--------|--------|--------|--------|--------|--------|---------|
| 0.01 | 1.07 | 1.01 | 0.97 | 0.94 | 0.93 | 0.93 | 0.94 | 0.95 |
| 0.10 | 0.96 | 0.96 | 0.95 | 0.95 | 0.95 | 0.95 | 0.95 | 0.95 |
| 0.50 | 0.98 | 0.98 | 0.98 | 0.98 | 0.98 | 0.98 | 0.97 | 0.97 |
| 1.00 | 1.00 | 1.00 | 0.99 | 0.99 | 0.99 | 0.99 | 0.99 | 0.99 |
| 2.00 | 1.30 | 1.29 | 1.29 | 1.29 | 1.28 | 1.28 | 1.28 | 1.28 |

Table 3: Median percentage error wrt the 95% Monte Carlo confidence interval for an Asian call IV under the fractional Bergomi ($H=0.2$) model.

at the behaviour of the linear approximation of the implied volatility. The methodology is the same as in the case of the SABR. The results are presented in Table 4 and Figure 11. Overall, the conclusion is the same as in the case of the SABR model. However, the approximation performs very well at short maturity ($T \leq 0.1$) around ATM region and gets worse with the increase of maturity. This impairment of the approximation is not drastic, but the error is bigger than in Monte Carlo simulation. One can see that the median error is bounded by 3.5 percent over the whole surface under consideration. This behaviour becomes clear by looking at Figure 12

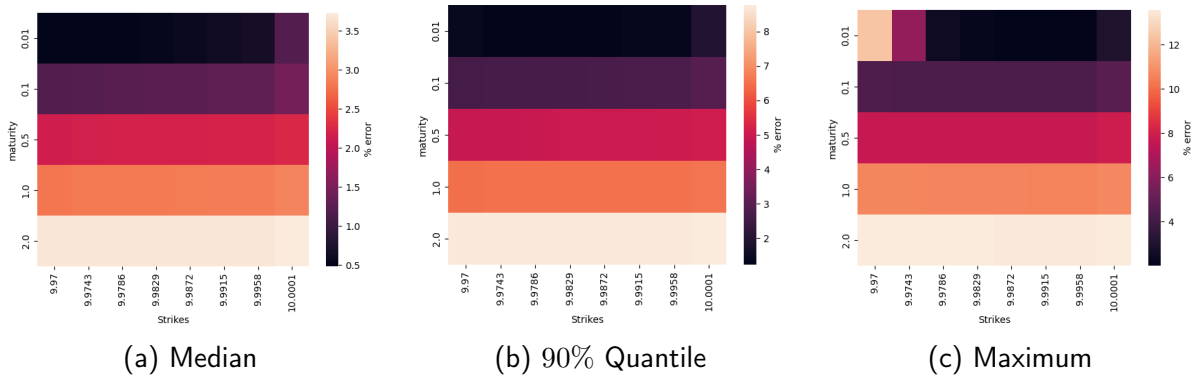


Figure 11: Accuracy of the approximation (9) for an Asian call IV under fractional Bergomi with $H = 0.2$.

Finally, we repeat our analysis in the case of the fractional Bergomi model with $H = 0.7$. The results are presented in Tables 5 and 6, Figures 13 and 14. One can see that the "typical" implied volatility surface in the sample is very close to the flat one. The level changes quite slowly as we move in the direction of moneyness and maturity. The curvature seems to be minimal if any. As a result, the linear approximation given by equation (9) works quite well in this case across different moneyness with maturity $T \leq 1$. This is quite different from the

| Maturity/Strike | 9.9700 | 9.9743 | 9.9786 | 9.9829 | 9.9872 | 9.9915 | 9.9958 | 10.0001 |
|-----------------|--------|--------|--------|--------|--------|--------|--------|---------|
| 0.01 | 0.49 | 0.50 | 0.50 | 0.54 | 0.59 | 0.64 | 0.67 | 1.19 |
| 0.10 | 1.17 | 1.21 | 1.23 | 1.25 | 1.26 | 1.28 | 1.29 | 1.46 |
| 0.50 | 2.16 | 2.18 | 2.19 | 2.19 | 2.19 | 2.20 | 2.20 | 2.26 |
| 1.00 | 2.80 | 2.82 | 2.83 | 2.83 | 2.84 | 2.85 | 2.85 | 2.90 |
| 2.00 | 3.68 | 3.68 | 3.69 | 3.69 | 3.69 | 3.69 | 3.69 | 3.73 |

(a) Median % error

| Maturity/Strike | 9.9700 | 9.9743 | 9.9786 | 9.9829 | 9.9872 | 9.9915 | 9.9958 | 10.0001 |
|-----------------|--------|--------|--------|--------|--------|--------|--------|---------|
| 0.01 | 1.41 | 1.28 | 1.25 | 1.24 | 1.29 | 1.33 | 1.34 | 1.93 |
| 0.10 | 2.61 | 2.64 | 2.68 | 2.67 | 2.69 | 2.72 | 2.72 | 2.93 |
| 0.50 | 4.92 | 4.93 | 4.96 | 4.98 | 5.00 | 5.00 | 5.02 | 5.07 |
| 1.00 | 6.50 | 6.51 | 6.52 | 6.52 | 6.52 | 6.52 | 6.51 | 6.57 |
| 2.00 | 8.72 | 8.74 | 8.74 | 8.74 | 8.74 | 8.74 | 8.74 | 8.77 |

(b) 90th quantile % Error

| Maturity/Strike | 9.9700 | 9.9743 | 9.9786 | 9.9829 | 9.9872 | 9.9915 | 9.9958 | 10.0001 |
|-----------------|--------|--------|--------|--------|--------|--------|--------|---------|
| 0.01 | 12.39 | 6.28 | 2.45 | 2.19 | 2.02 | 2.06 | 2.11 | 2.95 |
| 0.10 | 4.37 | 4.36 | 4.35 | 4.34 | 4.34 | 4.34 | 4.34 | 4.68 |
| 0.50 | 7.68 | 7.67 | 7.67 | 7.66 | 7.66 | 7.67 | 7.68 | 7.86 |
| 1.00 | 10.67 | 10.65 | 10.63 | 10.62 | 10.61 | 10.59 | 10.57 | 10.69 |
| 2.00 | 13.55 | 13.55 | 13.54 | 13.53 | 13.52 | 13.51 | 13.51 | 13.57 |

(c) Maximum % error

Table 4: Approximation error of an Asian call IV under the fractional Bergomi ($H=0.2$) model.

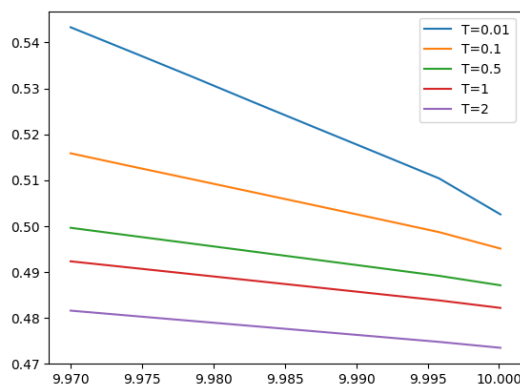


Figure 12: Typical surface of the IV of an Asian call under the fractional Bergomi ($H=0.2$) model.

behaviour that we observed in the case of the SABR and fractional Bergomi with $H = 0.2$.

| Maturity/Strike | 9.9700 | 9.9743 | 9.9786 | 9.9829 | 9.9872 | 9.9915 | 9.9958 | 10.0001 |
|-----------------|--------|--------|--------|--------|--------|--------|--------|---------|
| 0.01 | 0.91 | 0.90 | 0.90 | 0.90 | 0.91 | 0.92 | 0.93 | 0.94 |
| 0.10 | 0.92 | 0.92 | 0.92 | 0.93 | 0.93 | 0.93 | 0.94 | 0.94 |
| 0.50 | 0.94 | 0.94 | 0.94 | 0.94 | 0.94 | 0.94 | 0.94 | 0.94 |
| 1.00 | 0.95 | 0.95 | 0.95 | 0.95 | 0.95 | 0.95 | 0.95 | 0.95 |
| 2.00 | 0.99 | 0.99 | 0.99 | 0.99 | 0.99 | 0.99 | 0.99 | 0.99 |

Table 5: Median percentage error wrt the 95% Monte Carlo confidence interval for an Asian call IV under the fractional Bergomi ($H=0.7$) model.

| Maturity/Strike | 9.9700 | 9.9743 | 9.9786 | 9.9829 | 9.9872 | 9.9915 | 9.9958 | 10.0001 |
|-----------------|--------|--------|--------|--------|--------|--------|--------|---------|
| 0.01 | 0.32 | 0.30 | 0.28 | 0.27 | 0.27 | 0.26 | 0.27 | 0.74 |
| 0.10 | 0.39 | 0.36 | 0.33 | 0.31 | 0.31 | 0.31 | 0.30 | 0.46 |
| 0.50 | 0.61 | 0.62 | 0.64 | 0.65 | 0.68 | 0.72 | 0.74 | 0.82 |
| 1.00 | 1.34 | 1.36 | 1.37 | 1.42 | 1.42 | 1.42 | 1.45 | 1.50 |
| 2.00 | 3.28 | 3.27 | 3.25 | 3.25 | 3.25 | 3.27 | 3.32 | 3.38 |

(a) Median % error

| Maturity/Strike | 9.9700 | 9.9743 | 9.9786 | 9.9829 | 9.9872 | 9.9915 | 9.9958 | 10.0001 |
|-----------------|--------|--------|--------|--------|--------|--------|--------|---------|
| 0.01 | 0.84 | 0.77 | 0.70 | 0.65 | 0.62 | 0.59 | 0.56 | 1.19 |
| 0.10 | 1.08 | 0.97 | 0.88 | 0.81 | 0.74 | 0.68 | 0.63 | 0.79 |
| 0.50 | 2.06 | 1.93 | 1.79 | 1.68 | 1.55 | 1.45 | 1.47 | 1.54 |
| 1.00 | 3.56 | 3.44 | 3.32 | 3.26 | 3.22 | 3.17 | 3.15 | 3.16 |
| 2.00 | 7.59 | 7.60 | 7.56 | 7.65 | 7.64 | 7.63 | 7.62 | 7.51 |

(b) 90th quantile % Error

| Maturity/Strike | 9.9700 | 9.9743 | 9.9786 | 9.9829 | 9.9872 | 9.9915 | 9.9958 | 10.0001 |
|-----------------|--------|--------|--------|--------|--------|--------|--------|---------|
| 0.01 | 2.10 | 1.69 | 1.32 | 1.20 | 1.04 | 0.99 | 0.94 | 1.85 |
| 0.10 | 3.77 | 3.37 | 2.97 | 2.56 | 2.15 | 1.75 | 1.35 | 1.35 |
| 0.50 | 6.16 | 5.58 | 5.01 | 4.45 | 3.89 | 3.34 | 2.79 | 2.54 |
| 1.00 | 9.04 | 8.37 | 7.72 | 7.07 | 6.43 | 5.80 | 5.17 | 5.08 |
| 2.00 | 17.74 | 16.94 | 16.15 | 15.37 | 14.60 | 13.84 | 13.08 | 12.42 |

(c) Maximum % error

Table 6: Approximation error of an Asian call IV under the fractional Bergomi ($H=0.7$) model.

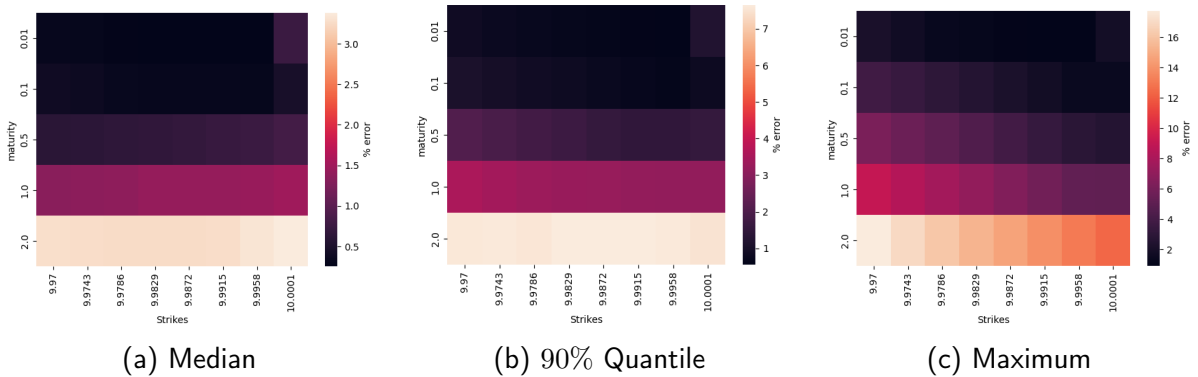


Figure 13: Accuracy of the approximation (9) for an Asian call IV under fractional Bergomi with $H = 0.7$.

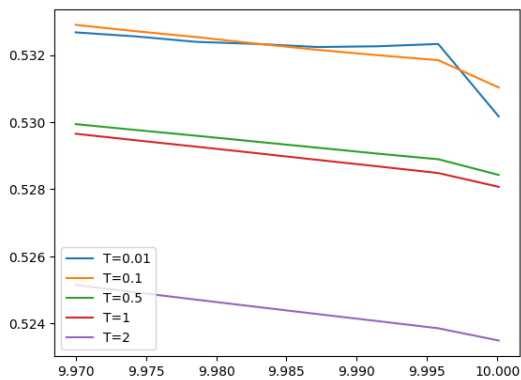


Figure 14: Typical surface of the IV of an Asian call under the fractional Bergomi ($H=0.7$) model.

5.3.2 European call option

We continue our analysis by repeating the calculations from the previous section in the case of the European call option. By contrast to the Asian case, now we are using Monte Carlo with 200000 paths and discretization step 0.02, $K = (9.0, 9.1, 9.2, \dots, 10)$. All the other parameters are set up in general are preserved.

The SABR Model We start by looking at the European call option under the Bachelier model with the SABR volatility. The implied volatility approximation accuracy using Monte Carlo is presented in Table 7. Next, we look at the behaviour of the implied volatility approx-

| Maturity/Strike | 9.0 | 9.1 | 9.2 | 9.3 | 9.4 | 9.5 | 9.6 | 9.7 | 9.8 | 9.9 | 10.0 |
|-----------------|------|------|------|------|------|------|------|------|------|------|------|
| 0.01 | 5.01 | 5.02 | 5.11 | 5.13 | 5.33 | 5.39 | 5.51 | 5.83 | 6.10 | 1.26 | 0.66 |
| 0.10 | 7.13 | 7.47 | 7.59 | 7.70 | 7.32 | 6.10 | 4.13 | 2.06 | 1.02 | 0.71 | 0.68 |
| 0.50 | 4.93 | 4.22 | 3.57 | 2.78 | 2.12 | 1.63 | 1.28 | 1.05 | 0.89 | 0.81 | 0.78 |
| 1.00 | 2.73 | 2.37 | 2.09 | 1.80 | 1.58 | 1.39 | 1.23 | 1.10 | 1.01 | 0.94 | 0.91 |
| 2.00 | 2.16 | 2.03 | 1.92 | 1.80 | 1.68 | 1.56 | 1.47 | 1.40 | 1.33 | 1.28 | 1.24 |

Table 7: Median percentage error wrt the 95% Monte Carlo confidence interval for the European call IV under the SABR model.

imation. The detailed results of the behaviour of different error types are presented in Table 8 and Figure 15. Overall, the approximation performs very well around ATM region and gets slightly worse with the increase of maturity. However, the approximation becomes very poor at the short end as we move away from the ATM region. This happens due to considerable curvature of the implied volatility in this region. This behaviour can be clearly seen at Figure 16, where we present "typical" surface for our simulated data set. As maturity increases, the curvature considerably decreases leading to the improvement of the approximation (9). Notice, that, by contrast to an Asian call option, ATM level of the implied volatility is much more stable making the approximation to work quite well as we increase the maturity of the option.

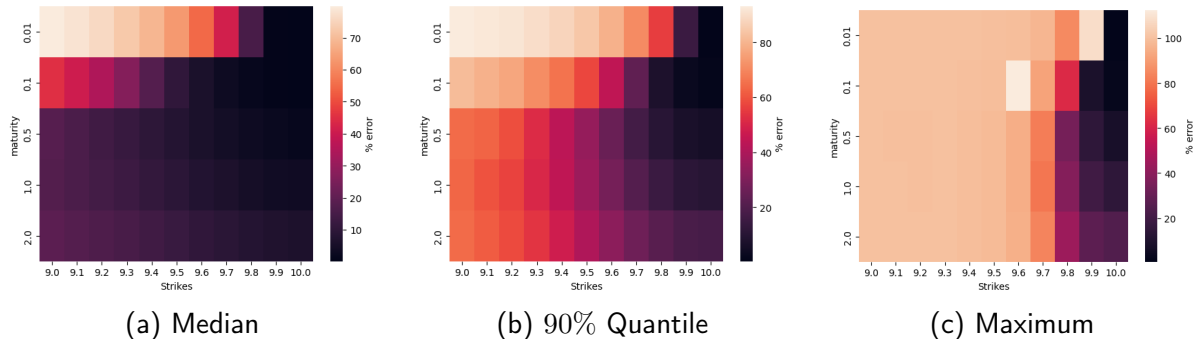


Figure 15: Accuracy of the approximation (9) for the European call under the SABR model.

fractional Bergomi Model We continue our analysis of the behaviour of the implied volatility approximation of the European call under the fractional Bergomi model. We start with the

| Maturity/Strike | 9.0 | 9.1 | 9.2 | 9.3 | 9.4 | 9.5 | 9.6 | 9.7 | 9.8 | 9.9 | 10.0 |
|-----------------|-------|-------|-------|-------|-------|-------|-------|-------|-------|------|------|
| 0.01 | 79.81 | 78.02 | 75.87 | 72.65 | 68.73 | 63.17 | 54.73 | 41.38 | 15.11 | 0.50 | 0.12 |
| 0.10 | 45.08 | 40.44 | 34.55 | 26.61 | 17.64 | 10.22 | 5.74 | 3.15 | 1.56 | 0.68 | 0.36 |
| 0.50 | 18.00 | 15.85 | 13.73 | 11.79 | 9.59 | 7.63 | 5.95 | 4.34 | 2.98 | 2.01 | 1.64 |
| 1.00 | 17.40 | 15.76 | 14.42 | 12.59 | 10.99 | 9.32 | 7.54 | 6.04 | 4.56 | 3.62 | 3.27 |
| 2.00 | 18.97 | 17.86 | 16.57 | 15.07 | 13.58 | 11.97 | 10.36 | 8.97 | 7.64 | 6.76 | 6.31 |

(a) Median % error

| Maturity/Strike | 9.0 | 9.1 | 9.2 | 9.3 | 9.4 | 9.5 | 9.6 | 9.7 | 9.8 | 9.9 | 10.0 |
|-----------------|-------|-------|-------|------|------|-------|-------|-------|-------|-------|-------|
| 0.01 | 93.11 | 92.30 | 91.62 | 89.5 | 87.3 | 84.13 | 79.02 | 70.72 | 55.43 | 14.58 | 0.30 |
| 0.10 | 81.61 | 79.17 | 76.51 | 71.2 | 65.8 | 57.31 | 44.07 | 23.27 | 7.53 | 2.52 | 1.18 |
| 0.50 | 64.29 | 62.99 | 58.69 | 51.7 | 43.1 | 34.75 | 25.43 | 16.92 | 10.34 | 6.54 | 5.44 |
| 1.00 | 63.31 | 59.60 | 56.81 | 50.3 | 44.7 | 36.31 | 28.17 | 20.67 | 14.55 | 11.11 | 10.05 |
| 2.00 | 64.19 | 61.34 | 58.16 | 53.6 | 47.7 | 40.42 | 33.17 | 26.61 | 21.58 | 18.42 | 17.45 |

(b) 90th quantile % Error

| Maturity/Strike | 9.0 | 9.1 | 9.2 | 9.3 | 9.4 | 9.5 | 9.6 | 9.7 | 9.8 | 9.9 | 10.0 |
|-----------------|-------|------|------|------|-------|------|-------|-------|-------|--------|-------|
| 0.01 | 99.9 | 99.9 | 99.9 | 99.9 | 99.8 | 99.6 | 99.1 | 96.6 | 84.89 | 108.34 | 0.60 |
| 0.10 | 99.8 | 99.8 | 99.8 | 99.8 | 99.4 | 98.8 | 112.3 | 91.5 | 62.06 | 8.82 | 2.10 |
| 0.50 | 99.79 | 99.6 | 99.6 | 99.7 | 98.9 | 98.2 | 94.5 | 81.98 | 34.07 | 14.22 | 8.1 |
| 1.00 | 99.75 | 99.7 | 99.6 | 99.7 | 99.1 | 97.9 | 94.8 | 80.43 | 38.08 | 19.46 | 14.27 |
| 2.00 | 99.76 | 99.7 | 99.7 | 99.8 | 99.19 | 98.1 | 95.0 | 83.84 | 44.11 | 27.61 | 24.3 |

(c) Maximum % error

Table 8: Approximation error of the European call IV under the SABR model.

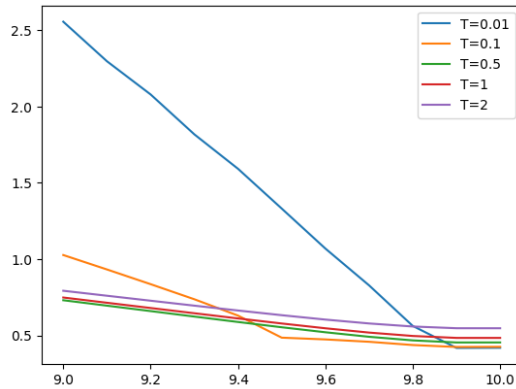


Figure 16: Typical surface of the IV of the European call under the SABR model.

case of $H = 0.2$ and present the accuracy of the Monte Carlo pricing at Table 9. Next, we move to the analysis of the behaviour of the implied volatility approximation (9). The detailed results regarding different error types are presented in Table 10 and Figure 18. To sum up, the behaviour of the implied volatility approximation is close to the SABR model. Similarly, the curvature of the implied volatility decreases considerably as options maturity increases. The stability of the ATM implied volatility level gives the improvement (except $T \leq 0.1$) in the quality of the linear approximation for a wide variety of options across all strikes and maturities. This behaviour can be clearly seen at Figure 17, where we present "typical" surface in

| Maturity/Strike | 9.0 | 9.1 | 9.2 | 9.3 | 9.4 | 9.5 | 9.6 | 9.7 | 9.8 | 9.9 | 10.0 |
|-----------------|------|------|------|------|------|------|------|------|------|------|------|
| 0.01 | 5.70 | 5.81 | 5.86 | 5.99 | 6.05 | 6.24 | 6.46 | 6.71 | 7.15 | 2.00 | 0.67 |
| 0.10 | 7.10 | 7.49 | 7.74 | 7.72 | 7.87 | 6.76 | 4.68 | 2.37 | 1.13 | 0.74 | 0.68 |
| 0.50 | 6.16 | 5.36 | 4.18 | 3.19 | 2.28 | 1.58 | 1.21 | 0.95 | 0.80 | 0.73 | 0.70 |
| 1.00 | 3.31 | 2.71 | 2.15 | 1.69 | 1.42 | 1.17 | 0.97 | 0.85 | 0.78 | 0.74 | 0.72 |
| 2.00 | 1.87 | 1.64 | 1.43 | 1.26 | 1.10 | 0.97 | 0.88 | 0.83 | 0.78 | 0.76 | 0.74 |

Table 9: Median percentage error wrt the 95% Monte Carlo confidence interval for the European call IV under the fractional Bergomi ($H=0.2$) model.

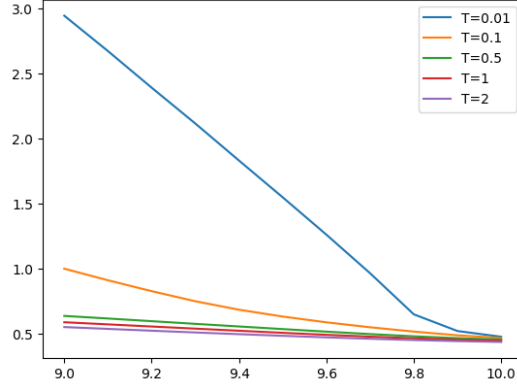


Figure 17: Typical surface of the IV of the European call under the fractional Bergomi ($H=0.2$) model.

our data set.

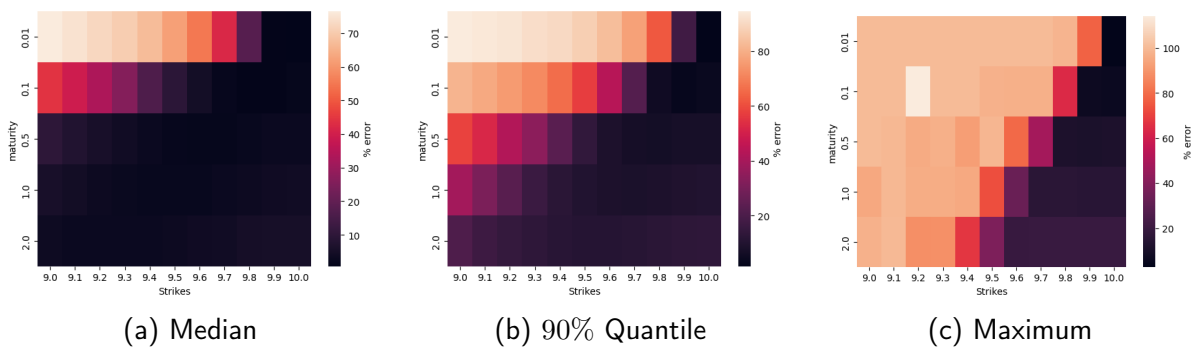


Figure 18: Accuracy of the approximation (9) for the European call under fractional Bergomi ($H=0.2$) model.

We conclude this section by looking at the approximation of the European call implied volatility under the fractional Bergomi model with $H = 0.7$. We present the accuracy of the Monte Carlo at Table 11. The detailed results regarding different error types are presented in Table 12 and Figure 20. Due to the equation (15) the implied volatility approximation in this case is a horizontal plane leveled at σ_0 . Visual justification of the flat skew can be clearly seen at Figure 19, where we present "typical" surface observed in our data set.

| Maturity/Strike | 9.0 | 9.1 | 9.2 | 9.3 | 9.4 | 9.5 | 9.6 | 9.7 | 9.8 | 9.9 | 10.0 |
|-----------------|-------|-------|-------|-------|-------|-------|-------|-------|-------|------|------|
| 0.01 | 76.52 | 74.74 | 72.48 | 70.59 | 67.12 | 61.92 | 54.90 | 42.06 | 17.64 | 1.09 | 0.64 |
| 0.10 | 44.01 | 39.03 | 33.18 | 25.90 | 16.32 | 9.26 | 4.73 | 1.97 | 0.98 | 1.06 | 1.53 |
| 0.50 | 9.72 | 7.38 | 5.62 | 4.08 | 2.77 | 2.04 | 1.76 | 1.78 | 2.17 | 2.75 | 2.99 |
| 1.00 | 5.39 | 4.22 | 3.30 | 2.64 | 2.24 | 2.19 | 2.35 | 2.74 | 3.15 | 3.80 | 3.96 |
| 2.00 | 3.37 | 2.90 | 2.86 | 2.83 | 2.95 | 3.28 | 3.64 | 3.98 | 4.82 | 5.15 | 5.25 |

(a) Median % error

| Maturity/Strike | 9.0 | 9.1 | 9.2 | 9.3 | 9.4 | 9.5 | 9.6 | 9.7 | 9.8 | 9.9 | 10.0 |
|-----------------|-------|-------|------|-------|-------|-------|-------|-------|-------|-------|------|
| 0.01 | 94.49 | 93.43 | 92.8 | 91.17 | 90.03 | 87.50 | 83.44 | 76.84 | 61.84 | 17.52 | 1.5 |
| 0.1 | 81.38 | 78.6 | 75.2 | 71.6 | 66.11 | 57.02 | 43.55 | 21.90 | 5.21 | 3.30 | 3.8 |
| 0.5 | 57.95 | 51.8 | 42.5 | 34.3 | 23.15 | 13.6 | 8.73 | 6.95 | 6.28 | 7.02 | 7.3 |
| 1.00 | 39.11 | 30.8 | 22.8 | 15.8 | 12.06 | 9.58 | 8.80 | 8.09 | 8.60 | 9.4 | 9.6 |
| 2.00 | 20.47 | 16.7 | 14.4 | 12.9 | 11.63 | 10.87 | 10.67 | 11.20 | 11.98 | 12.57 | 12.9 |

(b) 90th quantile % Error

| Maturity/Strike | 9.0 | 9.1 | 9.2 | 9.3 | 9.4 | 9.5 | 9.6 | 9.7 | 9.8 | 9.9 | 10.0 |
|-----------------|------|------|--------|-------|-------|-------|-------|-------|-------|-------|------|
| 0.01 | 99.9 | 99.9 | 99.95 | 99.86 | 99.97 | 99.97 | 99.81 | 99.73 | 98.30 | 77.47 | 2.8 |
| 0.10 | 99.8 | 99.8 | 113.99 | 99.81 | 99.74 | 97.15 | 97.02 | 96.83 | 63.78 | 6.46 | 5.8 |
| 0.50 | 99.8 | 98.8 | 95.42 | 96.90 | 92.12 | 98.48 | 79.16 | 48.12 | 11.34 | 11.06 | 11.4 |
| 1.00 | 94.7 | 99.2 | 96.14 | 95.76 | 95.07 | 72.91 | 32.94 | 15.38 | 14.98 | 14.8 | 14.7 |
| 2.00 | 97.4 | 99.4 | 88.06 | 88.41 | 67.31 | 38.39 | 19.24 | 19.54 | 19.58 | 19.50 | 19.3 |

(c) Maximum % error

Table 10: Approximation error of the European call IV under the fractional Bergomi ($H=0.2$) model.

| Maturity/Strike | 9.0 | 9.1 | 9.2 | 9.3 | 9.4 | 9.5 | 9.6 | 9.7 | 9.8 | 9.9 | 10.0 |
|-----------------|------|------|------|------|------|------|------|------|------|------|------|
| 0.01 | 4.26 | 4.35 | 4.27 | 4.24 | 4.89 | 4.39 | 4.87 | 4.92 | 3.79 | 0.86 | 0.66 |
| 0.10 | 5.88 | 5.99 | 6.68 | 6.41 | 5.67 | 4.25 | 2.30 | 1.03 | 0.71 | 0.64 | 0.66 |
| 0.50 | 4.93 | 3.95 | 2.91 | 2.10 | 1.45 | 1.07 | 0.86 | 0.74 | 0.68 | 0.67 | 0.67 |
| 1.00 | 2.76 | 2.23 | 1.74 | 1.37 | 1.14 | 0.95 | 0.83 | 0.75 | 0.72 | 0.70 | 0.70 |
| 2.00 | 1.86 | 1.62 | 1.41 | 1.22 | 1.07 | 0.96 | 0.89 | 0.84 | 0.80 | 0.78 | 0.77 |

Table 11: Median percentage error wrt the 95% Monte Carlo confidence interval for the European call IV under the fractional Bergomi ($H=0.7$) model.

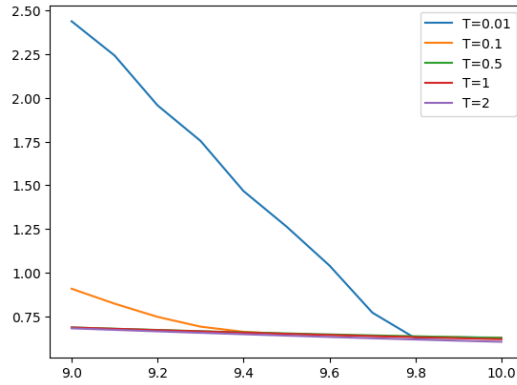


Figure 19: Typical surface of the IV of the European call under the fractional Bergomi ($H=0.7$) model.

| Maturity/Strike | 9.0 | 9.1 | 9.2 | 9.3 | 9.4 | 9.5 | 9.6 | 9.7 | 9.8 | 9.9 | 10.0 |
|-----------------|-------|-------|-------|-------|-------|-------|-------|-------|------|------|------|
| 0.01 | 78.96 | 76.27 | 73.63 | 70.05 | 65.67 | 59.42 | 49.13 | 34.11 | 5.86 | 0.69 | 0.11 |
| 0.10 | 42.65 | 36.66 | 29.48 | 20.49 | 11.22 | 6.98 | 4.47 | 3.02 | 1.95 | 0.98 | 0.16 |
| 0.50 | 14.28 | 12.76 | 10.69 | 9.22 | 7.60 | 6.29 | 5.17 | 3.80 | 2.47 | 1.27 | 1.21 |
| 1.00 | 13.16 | 11.85 | 10.62 | 9.17 | 8.05 | 6.64 | 5.35 | 3.88 | 2.94 | 2.69 | 3.13 |
| 2.00 | 12.59 | 11.37 | 10.41 | 9.18 | 7.85 | 6.89 | 6.35 | 6.23 | 6.70 | 7.92 | 8.26 |

(a) Median % error

| Maturity/Strike | 9.0 | 9.1 | 9.2 | 9.3 | 9.4 | 9.5 | 9.6 | 9.7 | 9.8 | 9.9 | 10.0 |
|-----------------|------|-------|------|-------|-------|-------|-------|-------|-------|-------|------|
| 0.01 | 88.6 | 87.53 | 85.8 | 83.93 | 81.58 | 78.05 | 73.05 | 64.31 | 47.62 | 5.37 | 0.2 |
| 0.10 | 69.5 | 66.35 | 62.5 | 57.49 | 50.85 | 41.63 | 28.34 | 10.56 | 5.41 | 2.83 | 0.4 |
| 0.50 | 40.1 | 34.09 | 28.9 | 23.43 | 19.74 | 16.83 | 14.13 | 11.52 | 8.27 | 5.03 | 2.9 |
| 1.00 | 31.4 | 28.42 | 26.1 | 24.08 | 22.49 | 20.28 | 17.70 | 15.02 | 11.88 | 8.7 | 7.6 |
| 2.00 | 31.2 | 29.55 | 29.4 | 29.37 | 29.09 | 28.46 | 26.44 | 24.34 | 21.68 | 19.55 | 19.5 |

(b) 90th quantile % Error

| Maturity/Strike | 9.0 | 9.1 | 9.2 | 9.3 | 9.4 | 9.5 | 9.6 | 9.7 | 9.8 | 9.9 | 10.0 |
|-----------------|------|-------|-------|------|-------|-------|------|-------|-------|-------|-------|
| 0.01 | 91.6 | 90.9 | 89.5 | 88.3 | 86.4 | 83.8 | 80.4 | 73.6 | 73.50 | 64.55 | 0.62 |
| 0.10 | 77.4 | 75.1 | 92.8 | 98.2 | 63.7 | 57.3 | 47.0 | 33.02 | 33.19 | 8.9 | 0.83 |
| 0.50 | 57.6 | 54.9 | 58.8 | 52.6 | 56.8 | 68.4 | 51.4 | 42.07 | 31.86 | 17.3 | 4.40 |
| 1.00 | 60.3 | 53.4 | 53.4 | 74.7 | 68.6 | 63.6 | 64.1 | 53.6 | 44.64 | 27.1 | 11.12 |
| 2.00 | 98.7 | 135.5 | 100.9 | 85.9 | 109.2 | 116.8 | 98.0 | 78.1 | 68.54 | 48.6 | 28.58 |

(c) Maximum % error

Table 12: Approximation error of the European call IV under the fractional Bergomi ($H=0.7$) model.

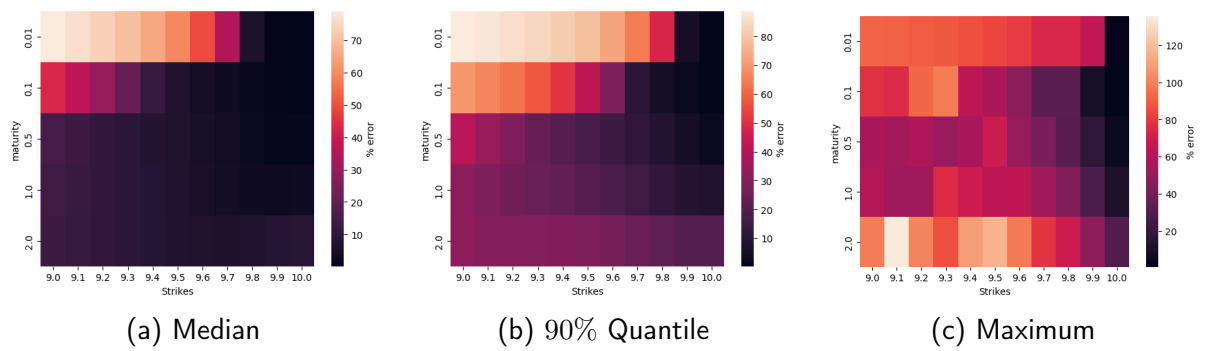


Figure 20: Accuracy of the approximation (9) for the European call under fractional Bergomi ($H=0.7$) model.

A A primer on Malliavin Calculus

We introduce the elementary notions of the Malliavin calculus used in this paper (see Nualart and Nualart [14]). Let us consider a standard Brownian motion $Z = (Z_t)_{t \in [0, T]}$ defined on a complete probability space $(\Omega, \mathcal{F}, \mathbb{P})$ and the corresponding filtration \mathcal{F}_t generated by Z_t . Let \mathcal{S}^Z be the set of random variables of the form

$$F = f(Z(h_1), \dots, Z(h_n)), \quad (17)$$

with $h_1, \dots, h_n \in L^2([0, T])$, $Z(h_i)$ denotes the Wiener integral of the function h_i , for $i = 1, \dots, n$, and $f \in C_b^\infty(\mathbb{R}^n)$ (i.e., f and all its partial derivatives are bounded). Then the Malliavin derivative of F , $D^Z F$, is defined as the stochastic process given by

$$D_s^Z F = \sum_{j=1}^n \frac{\partial f}{\partial x_j}(Z(h_1), \dots, Z(h_n)) h_j(s), \quad s \in [0, T].$$

This operator is closable from $L^p(\Omega)$ to $L^p(\Omega; L^2([0, T]))$, for all $p \geq 1$, and we denote by $\mathbb{D}_Z^{1,p}$ the closure of \mathcal{S}^Z with respect to the norm

$$\|F\|_{1,p} = \left(\mathbb{E} |F|^p + \mathbb{E} \|D^Z F\|_{L^2([0, T])}^p \right)^{1/p}.$$

We also consider the iterated derivatives $D^{Z,n}$ for all integers $n > 1$ whose domains will be denoted by $\mathbb{D}_Z^{n,p}$, for all $p \geq 1$. We will use the notation $\mathbb{L}_Z^{n,p} := L^p([0, T]; \mathbb{D}_Z^{n,p})$.

The following theorem is an extension of the classical Itô's Lemma for non-anticipating processes, see Proposition 4.3.1 in Alòs and García-Lorite [2].

Theorem 3 (Anticipating Itô's Formula). *Consider a process of the form*

$$X_t = X_0 + \int_0^t u_s dZ_s + \int_0^t v_s ds,$$

where X_0 is an \mathcal{F}_0 -measurable random variable and u and v are \mathcal{F}_t -adapted processes in $L^2([0, T] \times \Omega)$. Consider also a process $Y_t = \int_t^T \theta_s ds$, for some $\theta \in \mathbb{L}_Z^{1,2}$. Let $F : [0, T] \times \mathbb{R}^2 \rightarrow \mathbb{R}$ be a $C^{1,2}([0, T] \times \mathbb{R}^2)$ function such that there exists a positive constant C such that, for all $t \in [0, T]$, F and its derivatives evaluated in (t, X_t, Y_t) are bounded by C . Then it follows that for all $t \in [0, T]$,

$$\begin{aligned} F(t, X_t, Y_t) &= F(0, X_0, Y_0) + \int_0^t \partial_s F(s, X_s, Y_s) ds + \int_0^t \partial_x F(s, X_s, Y_s) u_s dZ_s \\ &\quad + \int_0^t \partial_x F(s, X_s, Y_s) v_s ds + \int_0^t \partial_y F(s, X_s, Y_s) dY_s \\ &\quad + \int_0^t \partial_{xy}^2 F(s, X_s, Y_s) u_s D^- Y_s ds + \frac{1}{2} \int_0^t \partial_{xx}^2 F(s, X_s, Y_s) u_s^2 ds, \end{aligned}$$

where $D^- Y_s = \int_s^T D_s^Z \theta_r dr$ and the integral $\int_0^t \partial_x F(s, X_s, Y_s) u_s dZ_s$ is defined in the Skorohod sense since the process $\partial_x F(s, X_s, Y_s) u_s$ is not adapted.

B The Price of an Asian Call Option under the Bachelier Model

In this section we prove the closed form formula for the price of an arithmetic Asian option under the constant volatility Bachelier model.

Theorem 4. Consider the model (1) in the case of constant volatility σ . Then, the price of an arithmetic Asian call option for $t \in [0, T]$ satisfies

$$B_A(t, S_t, y_t, k, \sigma) = \left(S_t \frac{T-t}{T} + \frac{y_t}{T} - k \right) N(d_A(k, \sigma)) + \left(\frac{\sigma(T-t)\sqrt{T-t}}{T\sqrt{3}} \right) n(d_A(k, \sigma)),$$

where

$$d_A(k, \sigma) = \frac{S_t \frac{T-t}{T} + \frac{y_t}{T} - k}{\left(\frac{\sigma(T-t)\sqrt{T-t}}{T\sqrt{3}} \right)},$$

T is the maturity, S_t is the stock price at time t , k is the strike price, and $y_t = \int_0^t S_u du$ is the state variable.

Proof. Firstly, notice the following representation

$$\begin{aligned} \frac{1}{T} \int_0^T S_t dt &= \frac{1}{T} \int_0^T \left(S_0 + \int_0^t \sigma dW_u \right) dt = S_0 + \frac{\sigma}{T} \int_0^T W_s ds = \\ &= S_0 + \frac{\sigma}{T} \int_0^t (T-s) dW_s + \frac{\sigma}{T} \int_t^T (T-s) dW_s. \end{aligned}$$

The last term on the right hand side is normally distributed with mean zero and variance equal to

$$\mathbb{E} \left(\frac{\sigma}{T} \int_t^T (T-s) dW_s \right)^2 = \frac{\sigma^2}{T^2} \int_t^T (T-s)^2 ds = \frac{\sigma^2 (T-t)^3}{3T^2}.$$

Due to the risk neutral pricing argument we know that

$$B_A(t, S_t, y_t, k, \sigma) = \mathbb{E}_t \left(\frac{1}{T} \int_0^T S_t dt - k \right)_+.$$

Therefore, using the above formulas this can be equivalently written as

$$\begin{aligned} \mathbb{E}_t \left(\frac{1}{T} \int_0^T S_t dt - k \right)_+ &= \mathbb{E}_t \left(S_t \frac{T-t}{T} + \frac{y_t}{T} - k + \frac{\sigma}{T} \int_t^T (T-s) dW_s \right)_+ = \\ &= \frac{1}{\sqrt{2\pi}} \int_{\frac{k-u_t}{z_t}}^{\infty} (u_t - k + z_t x) e^{-\frac{x^2}{2}} dx = \\ &= (u_t - k) N \left(\frac{u_t - k}{z_t} \right) + z_t n \left(\frac{u_t - k}{z_t} \right), \end{aligned}$$

where $u_t = S_t \frac{T-t}{T} + \frac{y_t}{T}$ and $z_t = \frac{\sigma(T-t)\sqrt{T-t}}{T\sqrt{3}}$.

The last step allows us to complete the proof. \square

References

- [1] Elisa Alòs. A generalization of the Hull and White formula with applications to option pricing approximation. *Finance and Stochastics*, 10(3):353–365, 2006.
- [2] Elisa Alòs, David García Lorite, and Dariusz Gatarek. *Malliavin Calculus in Finance*. Chapman and Hall/CRC, 2021.
- [3] Elisa Alòs, David García-Lorite, and Aitor Muguruza Gonzalez. On Smile Properties of Volatility Derivatives: Understanding the VIX Skew. *SIAM Journal on Financial Mathematics*, 13(1):32–69, 2022.

- [4] Elisa Alòs, Jorge A León, and Josep Vives. On the short-time behavior of the implied volatility for jump-diffusion models with stochastic volatility. *Finance and Stochastics*, 11(4):571–589, 2007.
- [5] Elisa Alòs, Eulalia Nualart, and Makar Pravosud. On the implied volatility of Asian options under stochastic volatility models. 2022.
- [6] L Bachelier. Théorie de la spéculation. *Annales scientifiques de l'École Normale Supérieure*, 3e série,:21–86, 1900.
- [7] Jaehyuk Choi, Minsuk Kwak, Chyng Wen Tee, and Yumeng Wang. A Black–Scholes user's guide to the Bachelier model. *Journal of Futures Markets*, 42(5):959–980, 2022.
- [8] José E Figueroa-López and Sveinn Ólafsson. Short-term asymptotics for the implied volatility skew under a stochastic volatility model with Lévy jumps. *Finance and Stochastics*, 20(4):973–1020, 2016.
- [9] Jean-Pierre Fouque, George Papanicolaou, and K Ronnie Sircar. From the implied volatility skew to a robust correction to Black–Scholes American option prices. *International Journal of Theoretical and Applied Finance*, 04(04):651–675, 2001.
- [10] Masaaki Fukasawa. Short-time at-the-money skew and rough fractional volatility. *Quantitative Finance*, 17(2):189–198, 2017.
- [11] Roza Galeeva and Ehud Ronn. Oil futures volatility smiles in 2020: Why the bachelier smile is flatter. *Review of Derivatives Research*, 25(2):173–187, 2022.
- [12] Jeffrey Ho Goodman, Laurie S. Interest Rates—Normal or Lognormal?, 2003.
- [13] Peter Jaeckel. Implied Normal Volatility. *Wilmott*, 2017:54–57, 2017.
- [14] David Nualart and Eulalia Nualart. *Introduction to Malliavin Calculus*. Cambridge University Press, 2018.
- [15] Walter Schachermayer and Josef Teichmann. How close are the option pricing formulas of Bachelier and Black–Merton–Scholes? *Mathematical Finance*, 18(1):155–170, 2008.
- [16] Satoshi Terakado. On the Option Pricing Formula Based on the Bachelier Model. *SSRN Electronic Journal*, 2019.